

A new metriacanthosaurid theropod dinosaur from the Middle Jurassic of Yunnan Province, China (#106452)

1

First submission

Guidance from your Editor

Please submit by **11 Oct 2024** for the benefit of the authors (and your token reward) .



Structure and Criteria

Please read the 'Structure and Criteria' page for guidance.



Custom checks

Make sure you include the custom checks shown below, in your review.



Author notes

Have you read the author notes on the [guidance page](#)?



Raw data check

Review the raw data.



Image check

Check that figures and images have not been inappropriately manipulated.

If this article is published your review will be made public. You can choose whether to sign your review. If uploading a PDF please remove any identifiable information (if you want to remain anonymous).

Files

Download and review all files from the [materials page](#).

15 Figure file(s)

3 Other file(s)

! Custom checks

New species checks



Have you checked our [new species policies](#)?



Do you agree that it is a new species?



Is it correctly described e.g. meets ICZN standard?




Structure and Criteria

Structure your review

The review form is divided into 5 sections. Please consider these when composing your review:

1. **BASIC REPORTING**
2. **EXPERIMENTAL DESIGN**
3. **VALIDITY OF THE FINDINGS**
4. General comments
5. Confidential notes to the editor






 You can also annotate this PDF and upload it as part of your review

When ready [submit online](#).





Editorial Criteria

Use these criteria points to structure your review. The full detailed editorial criteria is on your [guidance page](#).




BASIC REPORTING

-  Clear, unambiguous, professional English language used throughout.
-  Intro & background to show context. Literature well referenced & relevant.
-  Structure conforms to [Peerj standards](#), discipline norm, or improved for clarity.
-  Figures are relevant, high quality, well labelled & described.
-  Raw data supplied (see [Peerj policy](#)).

EXPERIMENTAL DESIGN

-  Original primary research within [Scope of the journal](#).
-  Research question well defined, relevant & meaningful. It is stated how the research fills an identified knowledge gap.
-  Rigorous investigation performed to a high technical & ethical standard.
-  Methods described with sufficient detail & information to replicate.

VALIDITY OF THE FINDINGS

-  **Impact and novelty is not assessed.** Meaningful replication encouraged where rationale & benefit to literature is clearly stated.
-  All underlying data have been provided; they are robust, statistically sound, & controlled.
-  Conclusions are well stated, linked to original research question & limited to supporting results.



The best reviewers use these techniques

Tip

Example

Support criticisms with evidence from the text or from other sources

Smith et al (J of Methodology, 2005, V3, pp 123) have shown that the analysis you use in Lines 241-250 is not the most appropriate for this situation. Please explain why you used this method.

Give specific suggestions on how to improve the manuscript

Your introduction needs more detail. I suggest that you improve the description at lines 57- 86 to provide more justification for your study (specifically, you should expand upon the knowledge gap being filled).

Comment on language and grammar issues

The English language should be improved to ensure that an international audience can clearly understand your text. Some examples where the language could be improved include lines 23, 77, 121, 128 - the current phrasing makes comprehension difficult. I suggest you have a colleague who is proficient in English and familiar with the subject matter review your manuscript, or contact a professional editing service.

Organize by importance of the issues, and number your points

1. Your most important issue
2. The next most important item
3. ...
4. The least important points

Please provide constructive criticism, and avoid personal opinions

I thank you for providing the raw data, however your supplemental files need more descriptive metadata identifiers to be useful to future readers. Although your results are compelling, the data analysis should be improved in the following ways: AA, BB, CC

Comment on strengths (as well as weaknesses) of the manuscript

I commend the authors for their extensive data set, compiled over many years of detailed fieldwork. In addition, the manuscript is clearly written in professional, unambiguous language. If there is a weakness, it is in the statistical analysis (as I have noted above) which should be improved upon before Acceptance.

A new metriacanthosaurid theropod dinosaur from the Middle Jurassic of Yunnan Province, China

Yi Zou^{1,2}, Li Chen³, Tao Wang⁴, Guo-Fu Wang³, Wei-Gang Zhang⁵, Xiao-Qin Zhang⁶, Zhen-Ji Wang⁶, Xiao-Chun Wu⁷, Hai-Lu You^{Corresp. 1, 2}

¹ Key Laboratory of Vertebrate Evolution and Human Origins, Institute of Vertebrate Paleontology and Paleoanthropology, Chinese Academy of Sciences, Beijing, China

² College of Earth and Planetary Sciences, Institute of Vertebrate Paleontology and Paleoanthropology, Chinese Academy of Sciences, Beijing, China

³ Chuxiong Prefectural Museum, Chuxiong, China

⁴ Center for Dinosaur Research and Protection, Bureau of Natural Resources of Lufeng City, Lufeng, China

⁵ Chuxiong Jurassic Cultural Tourism Industrial Park Development Co. Ltd, Chuxiong, China

⁶ Chuxiong Normal University, Chuxiong, China

⁷ Canadian Museum of Nature, Ottawa, Canada

Corresponding Author: Hai-Lu You
Email address: youhailu@ivpp.ac.cn

Metriacanthosaurid theropods represent a basal-branching lineage of tetanurans. Members of this clade are mainly medium to large-sized and lived in Laurasia during the Middle Jurassic to the Early Cretaceous. In this clade, *Sinraptor dongi*, *Sinraptor hepingensis*, and *Yangchuanosaurus shangyouensis* from the Late Jurassic are well represented by the nearly complete specimens, but the incompleteness of Middle Jurassic taxa hinders our knowledge of the origin and early evolution of Metriacanthosauridae. This paper describes a new genus and species of metriacanthosaurids, *Yuanmouraptor jinshajiangensis* gen. et sp. nov, from the Middle Jurassic Zhanghe Formation of Yunnan Province, China. The new taxon is represented by a cranium and the anterior section of the vertebral column including the complete cervical series and the first dorsal vertebra. *Yuanmouraptor jinshajiangensis* can be diagnosed based on the following autapomorphies: the anterior process of postorbital is sheet-shaped and keeps consistent depth; gently sigmoidal ventral ramus of postorbital with a laterally twisted trough running along it; processes on the anterodorsal margin of the third and fourth cervical neural spines; strongly posteriorly elongated epiphyses of anterior cervical vertebrae; deeply excavated pleurocoels on the third cervical vertebra; sheet-shaped and subrectangular neural spines of posterior cervical vertebrae. Phylogenetic analysis recovers *Yuanmouraptor* as the most basal-branching member within Metriacanthosauridae and provides a new alternative phylogenetic topology of non-coelurosaurian tetanurans.

1 **A new metriacanthosaurid theropod dinosaur from the**
2 **Middle Jurassic of Yunnan Province, China**

3

4 Yi Zou^{1,2}, Li Chen³, Tao Wang⁴, Guo-Fu Wang³, Wei-Gang Zhang⁵, Xiao-Qin Zhang⁶,
5 Zhen-Ji Wang⁶, Xiao-Chun Wu⁷, Hai-Lu You^{1,2}

6

7 ¹ Key Laboratory of Vertebrate Evolution and Human Origins, Institute of Vertebrate
8 Paleontology and Paleoanthropology, Chinese Academy of Sciences, Beijing, China

9 ² College of Earth and Planetary Sciences, University of Chinese Academy of Sciences,
10 Beijing, China

11 ³ Chuxiong Prefectural Museum, Chuxiong, China

12 ⁴ Center for Dinosaur Research and Protection, Bureau of Natural Resources of Lufeng
13 City, Lufeng, China

14 ⁵ Chuxiong Jurassic Cultural Tourism Industrial Park Development Co. Ltd., Chuxiong,
15 China

16 ⁶ Chuxiong Normal University, Chuxiong, China

17 ⁷ Canadian Museum of Nature, Ottawa, Canada

18

19 Corresponding Author:

20 Hai-Lu You¹

21

22

23 Email address: youhailu@ivpp.ac.cn

24

25 INTRODUCTION

26 Metriacanthosauridae is a family of medium-to-large sized carnivorous dinosaurs and represents a
27 basal-branching clade within the Allosauroidea (Holtz *et al.*, 2004; Smith *et al.*, 2007; Benson,
28 2010; Carrano *et al.*, 2012; Hendrickx *et al.*, 2015; Coria & Currie, 2016; Rauhut *et al.*, 2016,
29 2019, 2024; Lamanna *et al.*, 2020). Members of this clade mainly came from the Middle to Late
30 Jurassic strata of western China (Fig. 1), such as Sichuan, Chongqing, Xinjiang, and Yunnan
31 (Dong *et al.*, 1978, 1983; Gao, 1992, 1993, 1999; Currie & Zhao, 1993; Wu *et al.*, 2009). Apart
32 from these taxa found in China, metriacanthosaurid theropods were also reported in the Late
33 Jurassic of England (Huene, 1923; Walker, 1964), the Late Jurassic of Kyrgyzstan (Rauhut *et al.*,
34 2024), and the Early Cretaceous of Thailand (Buffetaut *et al.*, 1996). Recently, Yu *et al.* (2023)
35 reported the probable distribution of this clade in the Tibetan Plateau.

36 Here we report a new genus and species of Metriacanthosauridae collected from the Middle
37 Jurassic Zhanghe Formation of Jiangyi, Yuanmou county of Yunnan Province, China (Fig.1 B).
38 Material of this new taxon include a relatively complete skull and the first 11 vertebrae including
39 10 cervical vertebrae and the anterior-most dorsal vertebra. The Zhanghe Formation also yielded
40 sauropods including *Yuanmousaurus* (Lü *et al.*, 2006), *Eomamenchisaurus* (Lü *et al.*, 2008), and
41 *Nebulasaurus* (Xing *et al.*, 2015). Our phylogenetic analysis suggests that the new taxon is
42 probably one of the two most basal-branching metriacanthosaurids. Furthermore, some characters
43 present in the new taxon are also shared with several megalosauroids (Li *et al.*, 2009; Dai *et al.*,
44 2020) and non-tetanuran theropods (Colbert, 1989; Marsh & Rowe, 2020), which suggests that
45 these shared characters were gained independently by the aforementioned taxa.

46

47 MATERIAL & MATHODS

48 Material

49 The specimens studied here were excavated by a field team of Chuxiong Prefectural Museum from
50 a layer of red sandstones within the Zhanghe Formation at Jiangyi Town, Yuanmou County,
51 Chuxiong Yi Autonomous Prefecture, Yunnan, China in 2006, and is now on display in the
52 museum of Lufeng World Dinosaur Valley in Lufeng City, Yunnan Province. Most cranial bones
53 are still in articulation or closely associated. Some of the cranial elements are heavily distorted or
54 covered by matrix or other bones, rendering difficult or impossible to determine bone sutures or
55 internal structures. The specimen was prepared using mechanical tools (pneumatic chisels) and
56 photographed from various perspectives with a Sony DLSR-A700 digital camera. Line drawings
57 were made based on the reference photographs and checked against the original specimens.

58

59 **Phylogenetic analysis**

60 The new matrix for the phylogenetic analysis in this study was modified based on that of *Carrano*
61 *et al. (2012)*, which mainly focused on the phylogenetic relationship within tetanurans. We added
62 five new and 26 characters modified from the datasets of *Lamanna et al. (2020)*, *Eddy & Clark*
63 *(2011)*, *Brusatte & Serreno (2008)*, and *Schade et al. (2023)* (see the online Supplemental File S1
64 for details). We added the coelophysoid *Panguraptor (You et al., 2014)*, *Zuolong (Choiniere et al.,*
65 *2010)*, *Guanlong (Xu et al., 2006)*, and *Eoabelisaurus (Pol & Rauhut, 2012)* to the matrix to enrich
66 the samples of non-tetanurans, Coelurosauria, and Ceratosauria, respectively. Several basal-
67 branching tetanurans such as *Asfaltovenator (Rauhut & Pol, 2019)*, *Wiehenvenator (Rauhut et al.,*
68 *2016)*, and *Yunyangosaurus (Dai et al., 2020)* were added because these taxa were recently
69 reported tetanurans. *Alpkarakush kyrgyzicus (Rauhut et al., 2024)* (the most recently named
70 Central Asian metriacanthosaurid) was also added to the dataset. The new matrix, consisting of
71 372 characters and 70 operational taxonomic units (OTUs), was analyzed using TNT v. 1.6
72 (*Goloboff & Catalano, 2023*). The most parsimonious trees (MPTs) were recovered by a traditional
73 search of 1000 replicates of Wagner trees followed by tree bisection and reconnection, with 10
74 trees saved per replication. **Characters were equally weighted**, and none of the characters were
75 **treated as ordered.**

76

77 **Nomenclatural acts**

78 The electronic version of this article in Portable Document Format (PDF) will represent a
79 published work according to the International Commission on Zoological Nomenclature (ICZN),
80 and hence the new names contained in the electronic version are effectively published under that
81 Code from the electronic edition alone. This published work and the nomenclatural acts it contains
82 have been registered in ZooBank, the online registration system for the ICZN. The ZooBank
83 LSIDs (Life Science Identifiers) can be resolved and the associated information viewed through
84 any standard web browser by appending the LSID to the prefix <http://zoobank.org/>. The LSID for
85 this publication is: urn:lsid:zoobank.org:pub:2A9F32AD-B671-4F48-8A6E-0A69976A75FB.
86 The online version of this work is archived and available from the following digital repositories:
87 PeerJ, PubMed Central SCIE and CLOCKSS.

88

89 **RESULTS**

90 **Systematic paleontology**

91 Dinosauria *Owen, 1842*

92 Theropoda *Marsh, 1881*

93 Tetanurae *Gauthier, 1986*

94 *Allosauroidea* Currie & Zhao, 1993

95 *Metriacanthosauridae* Paul, 1988

96 *Yuanmouraptor* gen. nov.

97 **Diagnosis**—As for the only species.

98 *Yuanmouraptor jinshajiangensis* gen. et sp. nov.

99 **Etymology**—The genus name, ‘*Yuanmou*’, refers to Yuanmou County where the holotype was
100 collected, and ‘raptor’ is Latin for the robber. The specific name, ‘*jinshajiang*’ (the middle region
101 of Yangtze River) which passes through Yuanmou County and the type locality is located on the
102 north bank of the river.

103 **Holotype**—LFGT-ZLJ0115: a partial skeleton consists of a nearly complete skull with mandible
104 and 11 articulated anterior vertebrae including 10 cervical vertebrae and the first dorsal vertebra.

105 **Type Locality and horizon**—Jiangyi Town, Yuanmou County, Chuxiong Yi Autonomous
106 Prefecture, Yunnan Province, China; Zhanghe Formation, early Middle Jurassic,
107 Aalenian/Bajocian ((Bureau of Geology and Mineral Resources of Yunnan Province 1990).

108 **Diagnosis**—A medium-sized metriacanthosaurid dinosaur differing from other
109 metriacanthosaurids by the following unique combination of characters (autapomorphies are
110 indicated with an asterisk): ventral extension of antorbital fossa on maxilla is dorsoventrally deep,
111 which is shared with non-tetanurans, *Marshosaurus* and *Eocarcharia*, and some basal-branching
112 coelurosaurids such as *Ornitholestes* and *Proceratosaurus*; an accessory foramen located within
113 antorbital fossa on lacrimal and ventral to pneumatic foramen, similar to *Allosaurus*; dorsal part
114 of postorbital forming a very low rugosity, similar to megalosaurids; lack of pneumatic fenestra
115 on lateral surface of jugal, shared with non-tetanurans; the anterior process of postorbital sheet-
116 shaped and its depth keeping consistent*; gently sigmoidal ventral ramus of postorbital with a
117 laterally twisted trough running along it*; process on anterodorsal margin of the third and fourth
118 cervical vertebrae*; flattened peripheral band on anterior articular surface of anterior cervical
119 centra, shared with *Yunyangosaurus* and megalosaurids; strongly posteriorly elongated
120 epiphyses on anterior cervical vertebrae*; deeply excavated pleurocoels on the third cervical
121 vertebra*; sheet-shaped and subrectangular neural spines of posterior cervical vertebrae*.

122

123 **General description of the cranium**

124 The conditions of preservation of LFGT-ZLJ0115 are different between each side, and bones show
125 many fractures which might be caused during fluvial transportation. On the left side (Fig. 2 A B),
126 most parts of the nasal and elements around the orbit and lateral temporal fenestra are missing. On
127 the right side (Fig. 2 C D), although the nasal is also poorly preserved, other bones are relatively
128 more complete than those of the left side. The mandibular ramus is well-preserved on both sides.
129 The remnant elements of the skull and mandible are generally articulated, and thus most of the

130 internal structures are obscured from observation except the right ramus of the mandible. The main
131 fenestrae of the skull, such as the naris, antorbital fenestra, orbit, lateral temporal fenestra, and
132 supratemporal fenestra, are all damaged or largely distorted. The preserved skull is measured 53.9
133 cm in anteroposterior length, and the reconstruction (Fig. 3) of the skull measures 60.1 cm in
134 anteroposterior length. In comparison, the type specimen of *Yangchuanosaurus shangyouensis*
135 (Dong et al., 1978) bears a skull length of 78 cm, and the referred specimen (*Y. magnus*, reported
136 by Dong et al. [1983], was considered to present different ontogenetic stage of *Y. shangyouensis*
137 by Carrano et al. [2012]) has an estimated skull length of 111 cm. The skull of *Sinraptor dongi*
138 (Currie & Zhao, 1993) is 90 cm long and the skull of *S. hepingensis* (Gao, 1992, 1999) is 104 cm
139 long.

140 Based on the closed neurocentral suture, *Yuanmouraptor* is probably a mature individual.

141

142 **Premaxilla**—Only the left premaxilla (Fig. 4 A, B) is preserved, with most supranarial process
143 missing except for its risen base. In lateral view, the ~~outline of the~~ premaxillary body (below the
144 external naris) is roughly quadrangular and slightly higher than long (5.65×5.42 cm), with the
145 ventral border of the external naris is nearly paralleled with the premaxillary alveolar margin,
146 which is similar to the condition of *Ceratosaurus* (Madsen & Welles, 2000), *Torvosaurus* (Britt,
147 1991), *Majungasaurus* (Sampson & Witmer, 2007), and many allosauroids, such as *Sinraptor*
148 (Currie & Zhao, 1993; Gao, 1999), and *Acrocanthosaurus* (Eddy & Clarke, 2011), but in contrast
149 to *Sinraptor* (Currie & Zhao, 1993), *Allosaurus* (Britt, 1991), *Neovenator* (Brusatte et al., 2008),
150 *Dubreuillosaurus* (Allain, 2002), *Marshosaurus* (Madsen, 1976b), and *Monolophosaurus*
151 (Brusatte et al., 2010a), in which the premaxilla is slightly longer than high. The premaxilla is
152 much longer than high (length/height > 2) in spinosaurids like *Suchomimus* (Sereno et al., 1998)
153 and *Ceratosuchops* (Barker et al., 2021). The premaxilla of *Yuanmouraptor* bears four alveoli,
154 which is a primitive condition for theropods (Allain, 2002; Sampson & Witmer, 2007, Currie &
155 Zhao, 1993), as in *Sinraptor*, *Yangchuanosaurus*, but five alveoli are present in *Allosaurus* and
156 *Neovenator* (Brusatte et al., 2008). In spinosaurids, the number of alveoli could reach seven. The
157 fourth tooth is broken with only a little part of its base preserved. The other three are complete and
158 compress mediolaterally with slightly backward curvature. The distal carina is well-developed and
159 extended throughout the whole length, whereas the mesial carina is only visible at the epical one
160 third of the second tooth in lateral view (Fig. 4 C).

161 The anterodorsal border of the premaxillary body is missing, along with the main part of the
162 supranarial process (nasal process), but the preserved base of the process forms the anteroventral
163 margin of the external naris and indicates the posterodorsal orientation of the process. The narial
164 fossa is located ventrally to the remnant part of the external naris as in *Acrocanthosaurus*,
165 *Sinraptor*, *Allosaurus*, and *Dubreuillosaurus*. The complete portion of the anterodorsal rim

166 suggests that the anterior margin of the premaxillary body is nearly vertical as in *Sinraptor*,
167 *Ceratosaurus*, and *Allosaurus*, whereas that of *Torvosaurus*, *Dubreuillosaurus*, and *Duriavenator*
168 (*Benson, 2008*) is more rounded and more posterodorsally inclined. The subnarial process
169 (maxillary process) is relatively complete and of triangular-shape tapering posterodorsally in
170 lateral view, resembling that of *Ceratosaurus*, *Neovenator*, and *Sinraptor* in relative size and
171 orientation. The subnarial process in *Acrocanthosaurus* and *Allosaurus* is elongated
172 dorsoposteriorly, whereas in *Duriavenator* this process is horizontally elongated without the dorsal
173 inclination. The posteroventral rim of the subnarial process is confluent with the posterior border
174 of the premaxillary body, and both form the slightly posterodorsally inclined suture with the
175 maxilla in lateral view. The posterior border of the premaxillary body ventral to the subnarial
176 process presents a rugose surface and indicates the overlying of the maxilla (Fig. 4 B). There is no
177 evident subnarial foramen near the posterior border of the premaxillary body and subnarial
178 process, whereas the subnarial foramen is well developed in *Allosaurus*, *Acrocanthosaurus*,
179 *Sinraptor*, and other theropods. Based on the suture of the premaxilla with the maxilla, there is no
180 subnarial gap between these two bones, and the tooth row of each bone is continuous and at the
181 same level, as in most allosauroids.

182 Numerous foramina are mainly scattered on the lateral surface ventral to the mid height of the
183 premaxillary body and open ventrolaterally, similar to the distribution pattern in *Sinraptor* and
184 *Yangchuanosaurus*, whereas in many megalosaurids (*Dubreuillosaurus*, *Torvosaurus* and
185 *Marshosaurus*) the foramina are mainly distributed on the anterior half of the premaxillary body.
186 In *Neovenator*, the foramina spread evenly over the lateral surface of the premaxillary body.
187 Recent research (*Carr et al., 2017; Barker et al., 2017; Cullen et al., 2023*) proposed that these
188 foramina in terrestrial theropods probably house branches of trigeminal nerve linking to
189 integumentary sensory organs, which are related to foraging, intraspecific communication and nest
190 building behavior.

191

192 **Maxilla**—Both the left and right maxillae are adhered to the matrix, and thus the medial surface
193 is obscured. The main body of the left maxilla (Fig. 4 E, F) is well-preserved but lacks most of its
194 ascending ramus. The posterodorsally oriented base of the ascending ramus of the right maxilla
195 (Fig. 4 G, H) is preserved, but the anterodorsal margin of the lateral surface is missing. The
196 anteroposterior length of the preserved part of the left maxilla is measuring 28.87 cm, and the right
197 element is 29 cm.

198 On the lateral surface, the ventral wall of the external antorbital fossa is very developed, occupying
199 more than half of the maxillary body ventrally, as in *Masiakasaurus* (*Carrano et al., 2011*),
200 *Marshosaurus* (*Madsen, 1976b*), and many allosauroids (*Currie & Zhao, 1993; Dong et al., 1983;*
201 *Gao, 1999; Madsen, 1976a, Sereno & Brusatte, 2008*). This is different from the moderate range

202 of the antorbital fossa wall reaching nearly half depth of the maxilla body in *Afrovenator* (Sereno
203 *et al.*, 1994), *Acrocanthosaurus* (Eddy & Clark., 2011), *Neovenator* (Brusatte *et al.*, 2008), and
204 *Ceratosaurus* (Madsen & Welles, 2000). In contrast, the antorbital fossa has very limited exposure
205 on the maxillary body in *Torvosaurus* (Britt, 1991; Hendrickx & Mateus, 2014), *Wiehenvenator*
206 (Rauhut *et al.*, 2016), *Monolophosaurus* (Zhao & Currie, 1993; Brusatte *et al.*, 2010a), and some
207 Carcharodontosaurids (Sereno *et al.*, 1996; Coria & Salgado, 1995; Coria & Currie, 2006;
208 Brusatte & Sereno, 2007). Some abelisaurids even totally lack the antorbital fossa on the maxillary
209 body like *Majungasaurus* (Sampson & Witmer, 2007) and *Kryptops* (Sereno & Brusatte, 2008).
210 The border of the antorbital fossa is better preserved and well-defined by a rim on the left maxilla,
211 while this rim is less developed on the right maxilla due to compression. The antorbital fossa is
212 anteriorly extensive, whose anterior-most border reaches the 3rd alveolus, as in *Sinraptor* (Currie
213 & Zhao, 1993) and *Ceratosaurus* (Madsen & Welles, 2000), indicating a reduced anterior ramus.
214 Above the 3rd tooth the rim gently curves upward, forming a round anteroventral margin of the
215 antorbital fossa as in *Sinraptor* (Currie & Zhao, 1993), *Yangchuanosaurus* (Dong *et al.*, 1983),
216 *Ceratosaurus* (Madsen & Welles, 2000), *Marshosaurus* (Madsen, 1976b), and *Monolophosaurus*
217 (Brusatte *et al.*, 2010a). This contrasts with the squared anteroventral border of the antorbital fossa
218 in *Eocarcharia* (Sereno & Brusatte, 2008), *Acrocanthosaurus* (Eddy & Clarke, 2011), and
219 *Dubreuillosaurus* (Allain, 2002). Posteriorly this rim flattens gradually throughout the length of
220 the posterior ramus.

221 The preserved ascending ramus of the right maxilla preserves the anteroventral margin of the
222 external antorbital fenestra. From the ventral margin of the antorbital fenestra, the preserved
223 ascending ramus is measuring 6.95 cm. The angle between the main axis of the ascending ramus
224 and the jugal ramus of the maxilla is not very sharp, and about 60°. The lateral surface of the
225 ascending ramus of the right maxilla is too fragmentary to determine whether it is excavated by
226 pneumatic openings (Fig. 4 G, H).

227 Although the ascending rami are heavily damaged on both maxillae, traces of two openings at the
228 base of the ascending ramus are preserved. On the left maxilla, the anterior concavity on the
229 anterodorsal margin of the maxillary body is smooth, demarcates the ventral rim of the
230 promaxillary fenestra, and its anterior end is adjacent to the anteroventral margin of antorbital
231 fossa. The posterior one only preserves its rounded ventral half. On the right maxilla, the anterior
232 opening only preserves its posterior rim while the posterior one is nearly intact. These two
233 openings are separately interpreted as promaxillary fenestra and maxillary fenestra here based on
234 their relative placement (Witmer, 1997). The preserved portion of the promaxillary fenestra
235 indicates that it is larger than the maxillary fenestra, which resembles the condition in *Sinraptor*
236 (Currie & Zhao, 1993) and *Eocarcharia* (Sereno & Brusatte, 2008). Relatively large promaxillary
237 fenestra is regard as a synapomorphy of Metriacanthosauridae (Carrano *et al.*, 2012), in many other

238 theropod (*Allosaurus*, *Neovenator*, *Ceratosaurus*, *Dubreuillosaurus*: Currie & Zhao, 1993;
239 Brusatte et al., 2008; Madsen & Welles, 2000; Allain, 2002) the promaxillary fenestra is slit-
240 shaped and blocked by lateral wall of maxilla from lateral view. A discrete rounded promaxillary
241 fenestra is present in *Acrocanthosaurus* (Eddy & Clarke, 2011), *Marshosaurus* (Madsen, 1976b),
242 and some coelurosaurs (Xu et al., 2006; Brusatte et al., 2009). The promaxillary and maxillary
243 fenestrae seem to merge into one opening in Carcharodontosaurinae (Hendrickx et al., 2015).
244 The ventral margin of the maxilla is slightly convex, with one row of neurovascular foramina
245 aligning right above and in parallel with it, similar to those present in *Sinraptor* (Currie & Zhao,
246 1993), *Allosaurus* (Madsen, 1976a), and *Monolophosaurus* (Brusatte et al., 2010a), in contrast to
247 two rows of neurovascular foramina present in *Marshosaurus* (Madsen, 1976b), *Shaochilong*
248 (*Brusatte et al., 2010b*), and *Eocarcharia* (Serenó & Brusatte, 2008). The foramina dorsal to the
249 anterior four alveoli opens anteroventrally, then the orientation of subsequent foramina gradually
250 turns more posteroventrally. Each foramina opens ventrally into a depression but is less
251 extensively than the band-like depress in *Ceratosaurus* (Madsen & Welles, 2000). After the 10th
252 alveolus, the foramina merge into a discontinuous longitudinal groove.
253 12 and 10 functional teeth are preserved on the left and right maxilla, respectively. Based on the
254 vacant space, each maxilla is estimated to bear at least 14 alveoli, similar to the condition in many
255 Allosauroids (Currie & Zhao, 1993; Madsen, 1976a; Dong et al., 1983). Each tooth is
256 mediolaterally compressed and strongly curved backward. Both mesial and distal carinae are
257 serrated, and the well-preserved ninth maxillary tooth bears 15 and 20 denticles per 5 mm on the
258 distal and mesial carinae, respectively (Fig. 4 D). The distal carina continues to the base of the
259 crown, but the mesial carina reaches less than half length of the crown from the tip, which is a
260 common condition in theropod. Among these preserved functional teeth, the fourth tooth is the
261 biggest in both left and right maxillae and reach the axial length of 4.60 cm in left and 3.99 cm in
262 right. The 3rd tooth of the premaxilla, which is the biggest premaxillary tooth, is similar in size to
263 the first maxillary tooth, and manifests that the size of the teeth is continuous from the premaxilla
264 to the maxilla. This case differs from the noticeable reduction in size of the posterior premaxillary
265 teeth in Spinosauridae.

266

267 **Lacrimal**—The right lacrimal is preserved relatively complete (Fig. 5 A, B), whereas the left one
268 lacks most of its dorsal part (Fig. 2 A, B). The dorsoventrally height of the lacrimal is 12.08 cm.
269 The ventral ramus of lacrimal contacts the anterodorsal process of jugal, and forms most of the
270 anterior rim of the orbit. The transverse width of the ventral process constricts at its mid-height,
271 and expands anteroposteriorly through the rest ventral part until it sutures with jugal. The
272 posteroventral margin of antorbital fenestra is broken, so it impossible to determine whether the
273 lacrimal contacts the maxilla. The angle between disconnected ventral ramus of lacrimal and the

274 jugal ramus of maxilla is approximately 120° (Fig. 2 C, D), such a blunt angle might be caused by
275 the preservation. The anterior ramus lacks most of its anterior end, but the posterodorsal margin
276 of antorbital fenestra is preserved. The remnant base of the anterior ramus and ventral ramus meet
277 at an angle slightly more than 90° .

278 The ventral ramus is formed by two laminae as in most other tetanurans: the lateral and the medial.
279 The ridge defined by the boundary of these two laminae forms the posteroventral margin of the
280 antorbital fossa and continues to the jugal. The lateral lamina protrudes anteriorly into the
281 antorbital fenestra at the $2/3$ height of the ventral ramus, and separates the antorbital fossa on
282 lacrimal into dorsal and ventral part as in *Allosaurus* (Madsen, 1976a), *Monolophosaurus*
283 (*Brusatte et al., 2010a*), and *Acrocanthosaurus* (*Currie & Carpenter, 2000*). In contrast, in
284 *Torvosaurus* (*Britt, 1991*) the antorbital fossa is continuous on anterior and ventral ramus of
285 lacrimal.

286 The posterodorsal part of the lacrimal bears a small, blunt, triangular boss, which lengthened 2.23
287 cm with rugosity distributed on its dorsal and ventral lateral surface, proportionally larger than the
288 small boss seen in *Torvosaurus* (*Britt, 1991*), but much less prominent than the distinct lacrimal
289 horn of *Allosaurus* (*Madsen, 1976a*) and *Ceratosaurus* (*Madsen & Welles, 2000*). A weak flange
290 is right below the posterodorsal boss of lacrimal, resembling that of *Ceratosaurus* (*Madsen &*
291 *Welles, 2000*) and *Sinraptor* (*Currie & Zhao, 1993*). In many carcharodontosaurids
292 (*Acrocanthosaurus*, *Giganotosaurus*, *Mapusaurus*:*Eddy & Clarke, 2011*; *Coria & Salgado, 1995*;
293 *Coria & Currie, 2006*) this flange is more pronounced and forms a process, which marks the lower
294 limit of the eye socket.

295 Two pneumatic openings excavate the main posterodorsal body of the lacrimal, located at the
296 posterodorsal rim of antorbital fossa. And a third foramen is about 0.8 cm below the larger
297 posterior opening, and falls within the region of antorbital fossa. This combination of foramina is
298 also seen in *Allosaurus* (*Madsen, 1976a*).

299

300 **Jugal**—The anterodorsal border of jugal are broken on both left and right sides, so it is unclear
301 whether the jugal separates the maxilla and lacrimal and slightly contributes to the antorbital
302 fenestra. The remnant jugal is 17.42 cm long on left (Fig. 5 G, H) and 16.40 cm on right side (Fig.
303 5 C-F). The anterior ramus of jugal rises dorsally into the lacrimal ramus to contact the lacrimal,
304 and contributes to the anteroventral rim of orbit. Immediately posterior to the base of the anterior
305 ramus the postorbital ramus of jugal is 7.02 cm high from the bottom of orbit on the right side, and
306 contributes to the posteroventral margin of the orbit. The postorbital ramus rises abruptly, forms a
307 steep angle with the jugal body. These two rami result in an acute ventral margin of the orbit,
308 similar to the condition in *Sinraptor* (*Currie & Zhao, 1993*), *Yangchuanosaurus* (*Dong et al.,*
309 *1983*), and *Allosaurus* (*Madsen, 1976a*). Beneath the ventral rim of the orbit, the dorsoventral

310 depth of jugal is 3.3 cm on the left and 2.91 cm on the right.
311 Posteriorly, the quadratojugal ramus of jugal bifurcates into an upper branch overlapping the
312 anterior ramus of the quadratojugal and a lower branch lying below the quadratojugal as in most
313 theropod, but differs from the triradiate posterior ramus of *Sinraptor* (Currie & Zhao, 1993). In
314 better preserved right jugal (Fig. 5 D), the upper branch is slightly shorter than the lower branch,
315 which differs from the much shortened upper branch seen in *Allosaurus* (Madsen, 1976a) and
316 *Monolophosaurus* (Brusatte et al., 2010a). The quadratojugal ramus strongly turns upwards on the
317 right side, and results in the convex ventral rim of lateral temporal fenestra. This exaggerating
318 curvature is more likely the distortion caused by compression. In contrast, on the left side the
319 quadratojugal ramus curves slightly downwards near the tip of the upper and lower branches (Fig.
320 5 G, H).

321 The posteroventral rim of the antorbital fossa is well-developed on jugal, and the rim is demarcated
322 by a ridge which is continues onto the ventral ramus of lacrimal. At the base of this ridge, the
323 lateral surface of jugal is smooth, and differs from the pneumatic openings seen in *Sinraptor*
324 (Currie & Zhao, 1993) and *Monolophosaurus* (Brusatte et al., 2010a). Beneath the postorbital
325 ramus, near the bottom of the left jugal, the lateral surface is penetrated by a small and flat foramen
326 (Fig. 5 H), but this foramen is absent on the right side. This might be considered as break, but a
327 similar foramen is present in *Sinraptor*.

328

329 **Quadratojugal**—Both left and right quadratojugals are preserved, the left one (Fig. 5 C-F) is of
330 heavy damage on its lateral surface, while the right one (Fig. 5 I) lacks most of its dorsal ramus.
331 The quadratojugal is L-shaped in lateral view, and compressed mediolaterally as in most
332 theropods. The left quadratojugal is 11.88 cm long and 6.48 cm high, while the right one is 12.96
333 cm long and 0.73 cm thick.

334 In lateral view, the ventral margin of the quadratojugal is convex, similar to the condition in
335 *Ceratosaurus* (Madsen & Welles, 2000) and *Sinraptor hepingensis* (Gao, 1992, 1999). The
336 posterior end of the bone forms a triangular process oriented posteriorly. The lateral surface of the
337 quadratojugal is smooth, with a slight depression (Fig. 5 C, D) extending throughout the base of
338 the dorsal ramus and occupy roughly 2/3 ventral depth of the main body. The anterior process
339 tapers anteriorly and is wedged into the upper and lower branches of the posterior ramus of the
340 jugal. The anterior process extends to be level with the anterior border of the lateral temporal
341 fenestra, more anteriorly than those of *Allosaurus* (Madsen, 1976a) and *Sinraptor dongi* (Currie
342 & Zhao, 1993), but falls shorter than the condition in *Monolophosaurus* (Brusatte et al., 2010a).
343 The dorsal process is preserved on the left quadratojugal, but most of its external surface is broken.
344 The remnant dorsal process takes the form of triangular, and tapers dorsally. The articulation with
345 the squamosal is not definitive due to the latter's missing.

346 In the medial view, the posterior end of the quadratojugal bears slight rugosity, which might be
347 the contact with the quadrate as in *Allosaurus*. Anterior to this rugosity, a deep fossa excavates
348 into the posterior end with a rounded rim (Fig. 5 E, F), and the bony wall is thin as a lamina
349 corresponding to the concave lateral surface.

350

351 **Postorbital**—Only the right postorbital has been preserved, and lacks most distal part of its
352 posterior ramus (Fig. 6 A, B). In lateral view, the postorbital is T-shaped in outline consisting of
353 the orbital, posterior and ventral rami. The postorbital measures 9.83 cm in dorsoventrally height
354 and 6.17 cm in anteroposteriorly length from the orbital ramus to the broken base of the posterior
355 ramus.

356 The postorbital projects anteriorly to form a sheet-shaped process (Fig. 6 A, B), differing from the
357 prominent orbital boss as seen in other derived metriacanthosaurids (*Dong et al., 1978, 1983; Gao,*
358 *1992; Currie & Zhao, 1993; Rauhut et al., 2024*). From the beginning of the juncture of orbital
359 ramus and ventral ramus of the postorbital, the orbital ramus is 2.69 cm long. Through this planar
360 orbital ramus, the postorbital contacts the frontal medially, and forms the orbital roof along with
361 prefrontal, lacrimal and a slight part of frontal as in *Sinraptor* (*Currie & Zhao, 1993*) and
362 *Allosaurus* (*Madsen, 1976a*). In contrast, the frontal or prefrontal is excluded from the orbital rim
363 due to the postorbital-lacrimal articulation as in *Carcharodontosaurus* (*Sereno et al., 1996*) and
364 *Eocarcharia* (*Sereno & Brusatte, 2008*). The orbital ramus maintains a relatively constant
365 thickness with the deepest portion measured 0.99 cm. This constant thickness of the orbital process
366 of postorbital in *Yuanmouraptor* also differs from conditions in *Torvosaurus* (*Britt, 1991*) and
367 *Eustreptospondylus* (*Sadleir et al., 2008*), in which the orbital processes increase the dorsoventral
368 depth gradually backwards.

369 The ventral ramus of the postorbital is transversely widened and anteroposteriorly tapered to the
370 distal end, with a prominent lamina (Fig. 6 A-D) running along its posterior border, differing from
371 the U-shaped posterior rim of postorbital in many megalosauroids (*Torvosaurus;*
372 *Eustreptospondylus; Wiehenvenator. Britt, 1991; Sadleir et al., 2008; Rauhut et al., 2016*).
373 Through the ventral part of this lamina the postorbital contacts the postorbital ramus of jugal. The
374 upper half of the ventral ramus extends posteroventrally, then the lower half turns downwards with
375 its tip curves backwards, resulting in gently sigmoidal profile in lateral view. The anterior rim of
376 the ventral ramus is smooth and concave, and there is no evidence of any anteriorly projecting
377 intraorbital process which defines the ventral border of eyeball as in *Acrocantosaur* (*Eddy &*
378 *Clarke, 2011*), *Carcharodontosaurus* (*Sereno et al., 1996*), *Majungosaurus* (*Sampson & Witmer,*
379 *2007*). A shallow trough begins at the anterodorsal rim of the orbit, then twists to face laterally on
380 the ventral ramus and shallows ventrally, which is considered as an autapomorphy of
381 *Yuanmouraptor*.

382 The roof of the postorbital body expands laterally into a longitudinal ridge, ventral to which the
383 lateral surface of main body forms a shallow depression (Fig. 6 B). This longitudinal ridge
384 continues onto the posterior ramus of postorbital, and marks the lateral rim of the supratemporal
385 fossa. The remnant of posterior ramus is mediolaterally thin, and its cross section tapers
386 dorsolaterally to form the ridge. The posterior ramus is deflected at an angle of nearly 70° from
387 the posteroventrally pointed ventral ramus.

388 In dorsal view (Fig. 6 E, F), a medial process contacts frontal anteriorly and laterosphenoid
389 posteromedially, forms the anterolateral border of the supratemporal fenestra. Between the frontal
390 and laterosphenoid, this process also has a very limited contact with the lateral projection of
391 parietal, similar to the condition of *Sinraptor* (Currie & Zhao, 1993). The supratemporal fossa is
392 shown as a shallow, poorly-defined depression, and its anterior rim is formed by postorbital
393 together with frontal, parietal and laterosphenoid.

394

395 **Prefrontal**—The prefrontal is a small element located between lacrimal and frontal, partly lacks
396 its anterior end (Fig. 6 E, F). The remnant prefrontal measures 5.15 cm in length, 2.70 cm in
397 width and 1.88 cm in depth. Due to the damage, the prefrontal is displaced posteriorly relative to
398 frontal, and overlaps the mediodorsal surface of the lacrimal. The nasal is poorly preserved, thus
399 the articulation between the prefrontal and the nasal is not definitive.

400 In dorsal view, the frontal is sub-rhomboid in outline, and contacts lacrimal laterally and frontal
401 medially, but sutures of these articulations are all broken. The dorsal surface of prefrontal is planar
402 and smooth. The prefrontal's posterolateral rim, which contributes to the orbital roof, is slightly
403 rugose as in *Sinraptor* (Currie & Zhao, 1993), this rugosity might continue onto the lacrimal boss.
404 Unlike the fusion with other bones or lateral covering of the lacrimal in carcharodontosaurids and
405 ceratosaurs (Sereno *et al.*, 1996; Sereno & Brusatte, 2008; Sampson & Witmer, 2007), the
406 prefrontal of *Yuanmouraptor* is exposed laterally on the dorsal rim of orbit and forms a supraorbital
407 notch together with frontal, postorbital and lacrimal, a condition close to that in *Allosaurus*
408 (Madsen, 1976a), *Sinraptor* (Currie & Zhao, 1993), and *Monolophosaurus* (Brusatte *et al.*,
409 2010a).

410

411 **Frontal**—The paired frontals (Fig. 6 E, F) are wedge-shaped in outline in dorsal view, and
412 articulate each other through the suture on the midline, though the structure of this suture is
413 deformed due to the compressional distortion. Both left and right frontals are preserved, but lack
414 their anterior end, thus the articular surface with nasal is not definitive. The right frontal is
415 relatively complete, about twice as long as it is wide, and measures 10.82 cm in length and 5.77
416 cm in width. Whereas the left frontal lacks its posterolateral part.

417 In dorsal view, the frontal contacts the prefrontal anteromedially, the postorbital posterolaterally

418 and the parietal posteromedially. The frontal reaches its great mediolateral width at a point level
419 with its contact with the postorbital, resembling that in *Sinraptor* (Currie & Zhao, 1993) and
420 *Allosaurus* (Madsen, 1976a). In contrast, the frontal of *Eustreptospondylus* (Sadleir et al., 2008)
421 is widest at the supraorbital notch. Prior to the contact with the postorbital, the transverse width of
422 the frontal shrinks abruptly to contribute to the supraorbital notch, this also occurs in *Sinraptor*
423 and *Allosaurus*. At the anterior rim of the supraorbital notch, the frontal expands laterally to form
424 the contact with the prefrontal, then the frontal tapers anteriorly. The dorsal surface of the frontal
425 is smooth, and its posterolateral part was occupied by a poorly-defined shallow recess, which is
426 continues with the recess on the postorbital and contributes to the anterior rim of supratemporal
427 fossa. Although the suture between paired frontals is broken, there is no sign of a midline ridge as
428 displayed in *Shaochilong* (Brusatte et al., 2010b). Posteriorly, the suture with the parietal is
429 interdigitating medially and roughly straight laterally, resembles that of *Sinraptor*, *Allosaurus* and
430 *Shidaisaurus* (Wu et al., 2009).

431

432 **Parietal**—The paired parietals are fused, and lack most of their posterodorsal part (Fig. 6 E, F).
433 The remnant parietal is similar to that of *Sinraptor* (Currie & Zhao, 1993) and *Shidaisaurus* (Wu
434 et al., 2009) in outline, and measures 6.69 cm in length and 8.24 cm in width. In dorsal view, the
435 parietal contacts the frontal through an interdigitating suture anteriorly. Posterior to the contact
436 with the frontal, the parietal expands laterally to form two slender projections, contacting the
437 posterolateral part of frontal in transversely straight suture. The tips of these projections reach the
438 postorbital and overlap the laterosphenoid. The dorsal surface between the projections is dorsally
439 convex, and differ from the additional bone deposition which protrudes laterally into the
440 supratemporal fenestra as in *Sinraptor*. Behind these projections the parietal constricts
441 transversally and measures as 2.84 cm in width. Due to the serious damage present on the
442 posterodorsal part of the parietal, the existence of nuchal crest and the border between the parietal
443 and the supraoccipital is not definitive.

444

445 **Squamosal**—Only the right squamosal has been preserved (Fig. 7 A-E), but deviates strongly
446 from the original position, with its anterior and ventral end obscured by sediment. As in many
447 theropods, the squamosal of *Yuanmouraptor* comprises four processes: the anterior process
448 contacting the posterior ramus of the postorbital; the ventral process that extends ventrally to cover
449 the quadrate laterally and contact the ascending process of quadratojugal; the medial process
450 underlapping the parietal; and a posterior process that envelopes the paroccipital process
451 anterolaterally.

452 In dorsal view (Fig. 7 A, B), the preserved part of squamosal measures 6.24 cm in maximum length
453 and 6.62 cm in width. The dorsal surface of the squamosal is smooth and slightly concave, and

454 subtriangular in outline. The obscuration of the postorbital and sediment preclude the observation
455 of the medial border of the dorsal surface of the squamosal, which contributes to the posterolateral
456 rim of the supratemporal fenestra. The lateral rim of dorsal surface is demarcated by a ridge (Fig.
457 7 B) which extends posteriorly from the remnant of the anterior process then recurves medially at
458 the base of the posterior process. The articular surfaces for the parietal and the paroccipital together
459 form the posterior border of the squamosal (Fig. 7 D). The medial process protrudes
460 anteromedially and is slightly convex posteromedially. The coarse surface of the medial process,
461 which is not continuous with the dorsal surface of the bone, indicates its contact with the parietal.
462 Anteromedial to the posterior process, the articular surface for the tip of the paroccipital process
463 is posteriorly concave and dorsoventrally deep, then becomes posteriorly flat and constricts in
464 depth to continue onto the base of the medial process.

465 In lateral view (Fig. 7 E), the remnant anterior process measures 3.36 cm in length, bears evident
466 dorsal and ventral rim, and the former contributes to the border of the concavity on the dorsal
467 surface. The remnant ventral process measures 3.25 cm in depth and inclines anteroventrally.
468 Together the anterior and ventral processes of the squamosal form the posterodorsal rim of the
469 lateral temporal fenestra, these two processes are at an angle of broadly 70° . In contrast, this angle
470 is blunter in basal-branching tetanurans such as *Sinraptor* (Currie & Zhao, 1993), *Allosaurus*
471 (Madsen, 1976a), *Afrovenator* (Serenio et al., 1994), and *Eustreptospondylus* (Sadleir et al., 2008).
472 The tip of the posterior process projects 1.89 cm posteriorly from the main body of the squamosal,
473 and differs from the posteroventrally oriented posterior process of *Sinraptor* (Currie & Zhao,
474 1993), *Allosaurus* and *Monolophosaurus* (Brusatte et al., 2010a). The lateral surface of the
475 posterior process of the squamosal is rugose and pitted, might for the attachment of ligament.

476 In posterior view (Fig. 6 C, D), the squamosal is dorsoventrally deep along the contact with the
477 exoccipital, and reaches its maximum depth near the posterior process, but becomes shallow
478 toward its medial process. The bottom of the articulate surface for the paroccipital process is
479 concave ventrally, might houses the quadrate head.

480

481 **Quadrate**—Both the left and right quadrate are seriously damage, the former (Fig. 7. F-H) lacks
482 most of its dorsal part and the latter (Fig 2. D) only preserves partial pterygoid flange. The bottom
483 of the left quadrate is well-preserved, with measuring 4.69 cm in mediolateral width, and is
484 separated by an anteromedially oriented intercondylar sulcus into the entocondyle and the
485 ectocondyle (Fig. 7 H). The ectocondyle is larger, which is similar to the condition in *Allosaurus*,
486 but contrasts with that of *Eustreptospondylus* (Sadleir et al., 2008) and *Ceratosaurus* (Madsen &
487 Welles, 2000) in which the entocondyle is rather larger. The ectocondyle is 2.79 cm wide
488 mediolaterally while the entocondyle is 2.5 cm wide. The long axes of the ento- and ectocondyles
489 are anteromedially oblique in broadly same direction, but slightly more medially directed than the

490 degree of the intercondylar sulcus. The anterior end of each condyle is at approximately the
491 approximate level, which contrasts with the strongly anterior protruding entocondyle in
492 *Torvosaurus* (Britt, 1991) and *Eustreptospondylus*. In lateral view, both mandibular condyles
493 extend anteriorly to form a concavity dorsal to them, while the posterior rim of the remnant
494 quadrate is straight along the shaft.

495

496 **Palatine**—The incomplete left palatine is preserved (Fig. 7 I, J) and lacks most of its posterior
497 processes, with its medial surface obscured by matrix. Whereas the right palatine is present by a
498 bar-like bone, and its structure is impossible to identify. The palatine takes the form of a saddle,
499 with the central part of the bone is lowest in dorsoventral depth. As preserved the palatine is 11.23
500 cm long anteroposteriorly, 4.5 cm deep dorsoventrally at the vomeropterygoid process, and 2.64
501 cm deep at the waisted region of the main body.

502 The anterior vomeropterygoid and maxillary processes are preserved, together define the posterior
503 limit of the internal naris choana. The vomeropterygoid process lacks its distal end, and inclines
504 mediodorsally at its base, then becomes more anteriorly oriented, thus the medial rim of the coana
505 is concave laterally. The maxillary process is more robust than the vomeropterygoid process, and
506 extends anteriorly with a laterally convex surface. The articular surface with the maxilla of the
507 palatine is not definitive due to the damage. In lateral view, a shallow fossa is present at the base
508 of the maxillary process, immediately posterior to the internal naris choana. This fossa might mark
509 the pneumatic recess of palatine, but does not penetrate the surface of bone and lead to the inner
510 space as in *Sinraptor* (Currie & Zhao, 1993) and *Acrocathosaurus* (Eddy & Clarke, 2011). A
511 similar fossa is present in *Neovenator* (Brusatte et al., 2008), but it is located more posteriorly at
512 the juncture of the jugal and medial process.

513

514 **Supraoccipital**—The supraoccipital is seriously broken, with most of its dorsal part missing. The
515 preserved part of the supraoccipital (Fig. 8 A, B) is 2.73 cm deep dorsoventrally and 5.19 cm wide
516 transversely at its base. Despite the heavy damage, the preserved base of the supraoccipital
517 indicates a prominent ridge running on the midline, and flanked by a pair of vertical grooves.
518 Lateral to the paired grooves the bone extends posterolaterally and might continue onto the
519 probable nuchal crest of parietal. The base of the middle ridge is triangular in shape, tapers
520 dorsally, and expands transversely based on the dorsal fracture. The ventral rim of supraoccipital
521 makes a slight contribution to the dorsal border of the foremen magnum as in *Sinraptor* (Currie &
522 Zhao, 1993), *Acrocathosaurus* (Eddy & Clarke, 2011), *Monolophosaurus* (Zhao & Currie, 1993),
523 and *Piatnitzkysaurus* (Rauhut, 2004), and this contribution measures 0.83 cm in breadth. On the
524 left side of the base of the bone, there are two foramina penetrates the external surface, but on the
525 opposite side the surface is smooth. The symmetrical paired foramina positioned lateral to the

526 midline near the base of supraoccipital are generally referred as exits for external occipital vein
527 (*Currie & Zhao, 1993*), vena capitis dorsalis (*Coria & Currie, 2002; Rauhut, 2004; Brusatte &*
528 *Serreno, 2007; Eddy & Clarke, 2011*) or vena cerebialis media (*Sampson & Witmer, 2007*). The
529 asymmetrical foramina present in supraoccipital in *Yuanmouraptor* might be caused by pathology
530 or taphonomic process. The supraoccipital expands laterally at its ventral margin to contact
531 otoccipitals.

532

533 **Otoccipital (Exoccipital-Opisthotic)**—The main body of the exoccipital-opisthotic complex is
534 well-preserved, but the tips of left and right paroccipital processes are missing (Fig. 8 D, E). A
535 possible suture between the exoccipital and opisthotic is present. In all preserved vertebrae the
536 neural arch is attached to the centrum and the absence of neurocentral suture in most of them,
537 indicating that this individual is nearly mature or subadult, thus this suture-like boundary is more
538 likely caused by damage.

539 In posterior view (Fig. 8 D, E), the paired exoccipitals are separated by the supraoccipital above
540 the foramen magnum. Then the exoccipitals form the lateral and ventral margin of the foramen
541 magnum, and meet each other at a midline suture throughout the dorsal surface of the occipital
542 condyle. The foramen magnum is 2.47 cm transversely wide and 1.32 cm dorsoventrally high,
543 proportionally broader than that of *Sinraptor* (*Currie & Zhao, 1993*) and *Allosaurus* (*Madsen,*
544 *1976a*). The paroccipital process is posterolaterally directed, and slightly turns downwards,
545 contrasts more sharply downturned condition with *Sinraptor* (*Currie & Zhao, 1993*) and *Allosaurus*
546 (*Madsen, 1976a*). The ventral limit of the base of process levels with the bottom of the occipital
547 condyle, as in *Allosaurus*, *Sinraptor*, and *Piatnitzkysaurus* (*Rauhut, 2004*), but contrasts more
548 dorsally placed ventral base of the paroccipital process with *Dubreuillosaurus* (*Allain, 2002*),
549 *Eustreptospondylus* (*Sadleir et al., 2008*), and *Leshansaurus* (*Li et al., 2009*). A depressed area
550 (Fig. 8 C) lies between the paroccipital process and the base of occipital condyle, and houses three
551 foramina for cranial nerves. Among these foramina, the dorsal one is for the vagus (X) and
552 accessory (XI) cranial nerves, the medioventral one and the lateroventral one is for the two
553 branches of the hypoglossal nerve (XII). The ventral part of the exoccipital-opisthotic tapers
554 ventrally, and overlaps the basioccipital laterally at the boundary between the basioccipital and the
555 basisphenoid. The suture with the basioccipital extends from the base of the occipital condyle to
556 the basal tubera.

557 In lateral view (Fig. 9 A, B), the anterodorsal corner of the exoccipital-opisthotic is covered by the
558 prootic, and the exoccipital-opisthotic forms the posterior boundary of the fenestra ovalis
559 approximately ventral to the crista prootica. The posteroventral rim of the paroccipital process,
560 formed by the metotic strut, is strongly concave posteriorly, and separates lateral and posterior
561 surfaces of the braincase. The suture with the basisphenoid is posteroventrally inclined and slightly

562 posteriorly concave.

563

564 **Prootic**—The prootic is mainly exposed on the lateral surface (Fig. 9), and the right prootic is
565 better preserved than the left one, with a complete prootic pendant. The prootic contacts the
566 laterosphenoid anteriorly, and posterior to the contact a shallow recess is present. Ventral to the
567 suture with the laterosphenoid, a longitudinal groove runs through the ventral part of the prootic.
568 Approximately posterior to the groove, a single foramen penetrating the bone houses the cranial
569 nerve VII, differs from two openings for the cranial nerve VII in *Eustreptospondylus* (*Sadleir et*
570 *al., 2008*). The opening for trigeminal (V) nerve originates in the anterior-most part of the prootic
571 and is even bounded by the laterosphenoid anteriorly in many tetanurans such as *Sinraptor* (*Currie*
572 *& Zhao, 1993*), *Eustreptospondylus*, *Dubreuillosaurus* (*Allain, 2002*), *Monolophosaurus* (*Brusatte*
573 *et al., 2010a*), and *Piatnitzkysaurus* (*Rauhut, 2004*), but in *Yuanmouraptor* this part is obscured by
574 the sediment, preventing the further observation.

575 The prootic contact the exoccipital-opisthotic posteroventrally with a jagged suture. A prominent
576 crista prootica (Fig. 9 B) marks the posteroventral margin of the prootic. Above the crista prootica
577 the prootic is contiguous with the base of paroccipital process and overlaps the exoccipital-
578 opisthotic laterally. The prootic forms the anterior boundary of the fenestra ovalis with the
579 exoccipital-opisthotic forming the posteroventral boundary, approximately ventral to the crista
580 prootica. Anteroventral to the fenestra ovalis, a slight process sits at the boundary between the
581 exoccipital-opisthotic and basisphenoid, and protrudes posteroventrally, similar to that in
582 *Sinraptor*.

583 The ventral part of the prootic mainly overlaps the basisphenoid laterally with the prootic pendant,
584 and the space between the pendant and exoccipital-opisthotic is infilled by sediment.

585

586 **Basioccipital**—The basioccipital is mainly exposed in the posterior view (Fig. 8 D, E), and its
587 central ventral part is incomplete. The basioccipital occupies more than 60 percent of the occipital
588 condyle. The occipital condyle is evidently wider (3.28 cm) than tall (2.3 cm), with rounded and
589 smooth articular surface. Unlike in *Sinraptor* (*Currie & Zhao, 1993*), *Allosaurus* (*Madsen, 1976a*),
590 and *Eustreptospondylus* (*Sadleir et al., 2008*), the basioccipital of *Yuanmouraptor* does not
591 contribute to the foramen magnum, and the paired exoccipitals meet each other in the midline.
592 Ventral to the neck of the occipital condyle, a shallow fossa is present, and the surface below the
593 neck is posteriorly concave and smooth, but is not as well-defined as the subcondylar recess seen
594 in *Piatnitzkysaurus* (*Rauhut, 2004*). The ventral rim of the basioccipital on the right side probably
595 represent the basal tuber, though it is not very apparent due to the damage. The remnant basal tuber
596 is level with the ventral limit of exoccipital-opisthotic, in contrast to the unusual condition of
597 *Sinraptor*, in which the exoccipital-opisthotic extends significantly more ventrally than the basal

598 tubera. Differs from the relatively narrow width between the basal tubera in *Sinraptor*, *Allosaurus*,
599 and *Monolophosaurus* (Zhao & Currie, 1993), the transverse width across the basal tubera is
600 broader than the transverse diameter of the occipital condyle in *Yuanmouraptor*. The suture with
601 the basisphenoid is visible near the basal tubera and could only be observed on the right side.

602

603 **Basisphenoid**—The basisphenoid could be mainly observed on the right side (Fig. 9). Its ventral
604 structures such as the basisphenoid recess and the basipterygoid process are obscured by other
605 bones and sediment. In lateral view, the basisphenoid contacts the exoccipital-opisthotic through
606 a posteriorly curved suture. The suture with the basioccipital is visible on the tip of the basal tubera.
607 The dorsal part of the basisphenoid is overlapped by the prootic. Only the base of the cultriform
608 process is exposed, and the remnant of it is obscured by matrix.

609

610 **Laterosphenoid**—Both left and right laterosphenoids are preserved, but most of their ventral parts
611 are either damaged or obscured by matrix. The laterosphenoid forms the anterior wall of the
612 brancase, and is surrounded dorsally by the parietal, posteriorly by the prootic and laterally by the
613 postorbital. The contact with the forntal is not definitive due to the bloking of the surrounding
614 articulated bones. The laterosphenoid is visible in dorsal and laterodorsal views(Figs 6, 9), and
615 forms the anteromedial rim of the supratemporal fenestra.

616

617 **Dentary**—Dentaries are preserved on both left and right side, but their posterior boundaries are
618 broken, so the suture with the surangular and angular is not clear. The relatively complete right
619 dentary (Fig. 2 C, D) is 34.1 cm long and reaches minimum depth (4.17 cm) at the level of the
620 fourth alveolus. In lateral view, the main part of the upper margin is straight, but a step appears at
621 nearly the fourth dentary teeth leading to a slight dorsoventral expansion as in *Eustreptospondylus*
622 (*Sadleir et al., 2008*). In contrast to the square anteroventral rim of dentary in *Giganotosaurus*
623 (*Coria & Salgado, 1995*), the tip of the ventral rim of dentary in *Yuanmouraptor* is rounded. The
624 lower margin of the dentary is concave and inclines more ventrally at the 11th alveolus, posterior
625 to which the dentary body expands vertically throughout its posterior half length. An array of
626 slightly undulate neurovascular foramina (Fig. 10 A, B) excavates the external surface of the bone
627 below anterior seven tooth. Posterior to and level with these foramina, a longitudinal groove
628 extends from the 11th alveolus along the rest dentary and runs upward gradually. Several smaller
629 foramina scatter over the anteroventral margin of the lateral surface. The function of these
630 neurovascular foramina on the dentary might be the same as those on the premaxilla and maxilla.
631 Most of the left and the right dentaries adhere to the matrix or other bones, only a bit of medial
632 surface of the left dentary is observable but poorly-preserved (Fig. 2 D). Through this limit expose
633 of medial surface, two unfused interdental plates are preserved on the exposed medial surface, and

634 takes form of sub-triangular, as in *Sinraptor* (Currie & Zhao, 1993), *Dubreuillosaurus* (Allain,
635 2002), *Marshosaurus* (Madsen, 1976b), and *Eustreptospondylus* (Sadleir et al., 2008). Ventral to
636 the interdental plates a trough represents the paradental groove, which demarcates the ventral
637 border of the interdental plates. A replacement tooth occurs between these two interdental plates,
638 and an unerupted tooth is exposed on the broken surface near the damaged interdental symphysis,
639 exhibiting serrated distal carina. The Meckelian groove appears as a narrow trough on the remnant
640 dentary, and the foramina anterior to it as in *Sinraptor* (Currie & Zhao, 1993) and *Allosaurus*
641 (Madsen, 1976a) might be damaged.

642 The relatively well-preserved left dentary (Fig. 10. A, B) bears nine functional teeth, from gaps
643 among which, at least 14 alveoli are estimated. 14-17 teeth are present in other derived Late
644 Jurassic allosauroids such as *Sinraptor* (Currie & Zhao, 1993), *Yangchuanosaurus* (Dong et al.,
645 1983), and *Allosaurus* (Madsen, 1976a). Similar to the condition in maxillary teeth, the distal
646 carina of dentary teeth continues from the base to the tip while the mesial carina develops along
647 less than half of the teeth from the apex. The dentary teeth are generally smaller in size than
648 maxillary tooth with the largest dentary teeth measures 2.73 cm high. Dentary teeth also have
649 greater curvature than those of maxillary and premaxillary teeth.

650

651 **Splénial**—Only the right splénial is observable, and is poorly-preserved, with most of its anterior
652 part obscured by other elements and the posterior boundary damaged (Fig. 10 E, F). Caused by the
653 compression during burial, the bone covers the anterior end of the prearticular medially. The bone
654 forms a posteroventrally tapering process and its anteroventral rim is slightly concave and smooth.
655

656 **Surangular**—The left surangular (Fig. 10 C, D) are better preserved than the right one, while the
657 latter is heavily compressed dorsoventrally, and the anterior end of each one are obscured or
658 damaged (Fig. 2). The right surangular measures 27.26 cm anteroposteriorly, and its suture with
659 the dentary is not clear due to the compression.

660 Anterolateral to the contact with the articular, a longitudinal surangular ridge (Fig. 10 D) is present
661 approximately below the dorsal margin of the surangular. The ridge ends posteriorly with a dorsal
662 concavity, which laterally demarcates the lateral glenoid contacting the ectocondyle of the
663 quadrate. Posterior to the lateral glenoid the surangular forms a U-shaped notch deeper than the
664 lateral glenoid, which contributes to the retroarticular process together with the articular, and is
665 similar to but dorsoventrally deeper than that of *Sinraptor* (Currie & Zhao, 1993) and
666 *Acrocanthosaurus* (Eddy & Clarke, 2011). The posterolaterally opened posterior surangular
667 foramen is exhibited posteroventrally to the surangular ridge and ventrolaterally to the mandibular
668 joint, and a second foramen is found further anteriorly. This resembles that of *Sinraptor* but
669 contrasts with the condition in *Monolophosaurus* (Brusatte et al., 2010a), in which the surangular

670 ridge is absent and the posterior surangular foramen is roofed by an unexpanded and smooth
671 surface.

672 The surangular forms most of the dorsal and posterior rim of the external mandibular fenestra. At
673 the posteroventral corner of the external mandibular fenestra, the surangular is overlapped laterally
674 by the bony wall formed by the angular. Medially the surangular have a hook like process (Fig. 10
675 E, F), which forms an angle of nearly 60° with the long axis of the surangular and contacts the
676 prearticular ventrally (Fig. 11 C, D). The posterior rim of the hooked process extends laterally and
677 contributes to dividing the glenoid into two parts. In medial view (Fig. 10 E, F), the surangular
678 thickens transversely to form a bar like dorsal rim, which demarcates the dorsal limit of the
679 adductor fossa. The M. adductor mandibulae externus is estimated to attach the concave surface
680 between this bar and the surangular ridge.

681

682 **Angular**—The left angular lacks most of its anterior part (Fig. 10 C, D), and the right angular is
683 strongly dorsoventrally compressed. The angular forms the posteroventral part of the mandible, it
684 thins dorsally to cover the surangular, and thickens ventrally to overlap the ventral margin of the
685 prearticular, which forms the ventral border of the adductor fossa. The angular is dorsally concave,
686 and forms the ventral rim of the external mandibular foramen. The remnant angular reaches the
687 maximum depth at its central part of the contact with the surangular.

688

689 **Prearticular**—The right prearticular could be observed in medial view (Fig. 10 E, F). The bone
690 is a ventrally bowed element, it dorsoventrally flares at its anterior and posterior ends, but
691 constricts in depth at its central part. The medial surface of the remnant prearticular is obscured by
692 angular anteriorly and surangular posteriorly. The anterior part of the ventral rim of the prearticular
693 is surrounded ventrally by the thickened angular. Whereas posterior to the contact with the angular,
694 the ventral rim of the angular is exposed in lateral view as in *Sinraptor* (Currie & Zhao, 1993) and
695 *Acrocanthosaurus* (Eddy & Clarke, 2011). The posterodorsal part of the prearticular forms a
696 dorsomedially directed triangular process, which contacts the hooked process of surangular
697 dorsolaterally (Fig. 11 C, D). Posterior to this process the prearticular forms a dorsally concave
698 embayment, which houses the articular.

699

700 **Articular**—The right articular is well-preserved and still in articulation with the prearticular and
701 surangular (Fig. 11). The retroarticular process is well-developed and has a concave dorsal surface,
702 which is dorsally oriented and bordered by sharp ridge, in contrast, this surface faces more
703 posteriorly in *Allosaurus* (Madsen, 1976a) and *Acrocanthosaurus* (Eddy & Clarke, 2011). In
704 lateral view (Fig. 11 A, B), the lateral rim of the retroarticular process surpasses the lateral wall of
705 the surangular and exposes laterally. In dorsal view, the posterior end of the retroarticular process

706 is U-shaped in outline, then the process constricts its lateral rim abruptly and then expands medially
707 at its anterior part, forming a lateral notch and a medial blunt process. This medial blunt process
708 is contiguous with the medial rim of the medial glenoid, and the opening for the chorda tympani
709 penetrates it from its posterodorsal surface to its ventral surface. Anteriorly a prominent ridge
710 separates the medial glenoid and retroarticular process as in *Sinraptor* (Currie & Zhao, 1993), this
711 ridge is more eminent in *Acrocanthosaurus* (Eddy & Clarke, 2011).

712

713 **General description of the axial skeleton**

714 All vertebrae are well-preserved but none of them bears a rib. Of them the first 10 vertebrae were
715 considered as belonging to the cervical series and the 11th was speculated to be the first dorsal
716 vertebra based on the common condition of 10 cervical vertebra in basal-branching tetanurans
717 (Holtz *et al.*, 2004) and the diapophysis of the eleventh vertebra that is more laterally expanded
718 than the preceding one as is the case in *Sinraptor* (Currie & Zhao, 1993) and *Yangchuanosaurus*
719 (Dong *et al.*, 1983). The neurocentral suture is only partly visible on the eighth and ninth cervicals,
720 indicating that this individual is an adult or subadult.

721

722 **Atlas-Axis**—In the atlas-axial complex (Fig. 12), the atlantal intercentrum is in articulation with
723 the axial intercentrum and odontoid. The proximal parts of both the left and right neurapophyses
724 are still attached to the atlantal intercentrum and are positioned laterally to the neural canal. There
725 is no evident prezygopophysis on the neurapophysis, indicating the absence of the proatlas as in
726 *Sinraptor* (Currie & Zhao, 1993). The exposed part of the atlantal intercentrum is similar to that
727 of *Shidaisaurus* (Wu *et al.*, 2009) and *Sinraptor* (Currie & Zhao, 1993). In anterior view, the main
728 body of the atlantal intercentrum is slightly wider than deep. The ventrolateral rim is slightly
729 convex, and the ventral rim becomes flat, resulting a sub-rectangular profile of the lower half. The
730 anterior articular surface is concave, for the articulation with the occipital condyle. The dorsal rim
731 of the atlantal intercentrum is ventrally depressed and underlaps the rounded ventral part of
732 odontoid.

733 The odontoid adheres to the upper half of the anterior articular surface of the axial centrum, and
734 its boundaries with the atlantal intercentrum and axial centrum are visible. The odontoid is divided
735 into a dorsal and an anterior surface by an anteriorly convex rim, and this rim is approximately
736 parallel with the ventral border which contacts the atlantal intercentrum. The dorsal surface of
737 odontoid is dorsally concave and continuous with the floor of the neural canal. The anterior surface
738 arches anteriorly to pass through the dorsal margin of the atlantal intercentrum. A single shallow
739 recess is located laterally on each side of the anterior surface of the odontoid, which differs from
740 the foramina penetrating the same position as these recesses in *Neovenator* (Brusatte *et al.*, 2008).
741 In anterior view the odontoid is in shape of semicircle, similar to the condition in *Allosaurus*

742 (*Madsen, 1976a*) and *Monolophosaurus* (*Zhao et al., 2009*).

743 The axial intercentrum is not observable in anterior view (Fig. 11 C) due to the obscuration of the
744 articulated atlantal intercentrum. In lateral view (Fig. 11 E), the axial intercentrum tapers
745 posterodorsally to form a sub-triangular lateral outline as in *Neovenator* (*Brusatte et al., 2008*),
746 *Piatnitzkysaurus* (*Bonapart, 1986*), and *Yunyangosaurus* (*Dai et al., 2020*). In contrast, the axial
747 intercentrum maintains a constant anteroposterior thickness dorsoventrally, resulting a sub-
748 rectangular outline in lateral view in *Sinraptor* (*Currie & Zhao, 1993*) and *Ceratosaurus* (*Madsen*
749 *& Welles, 2000*). The suture between the axial intercentrum and centrum is slightly inclined
750 anteroventrally, similar to the condition present in *Sinraptor* (*Currie & Zhao, 1993*), but in contrast
751 with nearly vertical suture in *Allosaurus* (*Madsen, 1976a*), *Neovenator* (*Brusatte et al., 2008*),
752 *Piatnitzkysaurus* (*Bonapart, 1986*), and *Yunyangosaurus* (*Dai et al., 2020*). The ventral surface of
753 the axial intercentrum is flat and ventrally faced, continuous with the ventral surface of the axial
754 centrum in lateral view as in *Ceratosaurus* (*Madsen & Welles, 2000*), *Dilophosaurus* (*Marsh &*
755 *Rowe, 2020*), *Majungasaurus* (*O'Connor, 2009*), *Piatnitzkysaurus* (*Bonaparte, 1986*), and
756 *Yunyangosaurus* (*Dai et al., 2020*), but differs from *Sinraptor* (*Currie & Zhao, 1993*),
757 *Monolophosaurus* (*Zhao et al., 2009*), *Neovenator* (*Brusatte et al., 2008*), and *Acrocanthosaurus*
758 (*Harris, 1998*), in which the ventral surface of the axial intercentrum is nearly horizontal. In ventral
759 view (Fig. 11 B), the suture between the intercentrum and centrum is well exposed and arches
760 anteriorly.

761 The axial centrum is longer ventrally than it is dorsally, a similar condition in *Sinraptor* (*Currie &*
762 *Zhao, 1993*). The anterior articular surface is mostly obscured by the odontoid and axial
763 intercentrum. The posterior articular surface is strongly concave, and is as approximately wide as
764 high. In lateral view, the ventral rim of the centrum strongly arches dorsally, and forms an acute
765 angle with the posterior articular surface as in *Sinraptor* (*Currie & Zhao, 1993*). The diapophysis
766 is located at the base of the neural arch, just above the centrum, and is present as a lateroventrally
767 oriented pedicle. Anteroventral to the diapophysis the parapophysis protrudes posteroventrally to
768 form a diminutive hump. The lateral surface of centrum is smooth and there is no trace of any
769 pneumatic structure. This contrasts with many allosauroids (*Currie & Zhao, 1993; Brusatte et al.,*
770 *2008; Harris, 1998*), in which pleurocoels invade the main body of the centrum ventral to the
771 diapophysis. The central part of the centrum tapers its transverse width downwards, resulting an
772 mediolaterally narrow and flat ventral surface as is the case in *Yunyangosaurus* (*Dai et al., 2020*).
773 This differs from the centrum that bears pronounced ventral keel in *Acrocanthosaurus* (*Harris,*
774 *1998*). The transversely narrow and ventrally tapering ventral surface of axial centrum without
775 ventral keel was considered as an autopomorphy of *Yunyangosaurus* (*Dai et al., 2020*).

776 The prezygopophyses are obscured by neurapophyses on both left and right sides (Fig. 11 E, F).
777 The postzygopophyseal facets of the axial centrum are well-developed, comparable in size to those

778 of postaxial cervicals. The V-shaped intrapostzygopophyseal lamina (tpol) medially connects
779 paired postzygopophyses dorsal to the neural canal. The developed epiphysis extends
780 posterodorsally from the distal end of the postzygopophysis and curves laterally. A well-developed
781 axial epiphysis also occurs in *Shidaisaurus* (Wu et al., 2009), *Sinraptor* (Currie & Zhao, 1993).
782 The neural spine is transversely thin and posterodorsal inclined. In lateral view, the neural spine
783 deflects at an angle of 50° with the neural canal throughout its ventral half, then the degree of
784 inclination decreases abruptly in rest dorsal part. This transition in the degree of deflection is
785 probably caused by breakage. Prior to the base of neural spine, a rounded eminence rises dorsally,
786 similar to the condition in *Neovenator* (Brusatte et al., 2008) and *Yunyangosaurus* (Dai et al.,
787 2020). The anterior end of the neural spine is positioned posterior to the anterior margin of the
788 neural canal, this contrasts the strongly anteriorly flared neural spine in *Dilophosaurus* (Marsh &
789 Rowe, 2020). The spinopostzygopophyseal lamina expands laterally from the neural spine and fills
790 the space between its summit and the epiphysis, resembling that of *Sinraptor* (Currie & Zhao,
791 1993; Gao, 1993, 1999), *Yangchuanosaurus* (Dong et al., 1983), *Dilophosaurus* (Marsh & Rowe,
792 2020), and *Yunyangosaurus* (Dai et al., 2020). In posterior view (Fig. 11 D), an anteriorly
793 excavated and subtriangular fossa is surrounded by the spinopostzygopophyseal lamina and
794 postzygopophyses, such fossa also occurs in *Sinraptor* (Currie & Zhao, 1993; Gao, 1992, 1999),
795 *Yangchuanosaurus* (Dong et al., 1983), *Ceratosaurus* (Madsen & Welles, 2000), and
796 *Dilophosaurus* (Marsh & Rowe, 2020).

797

798 **Postaxial vertebrae**—The third to fifth cervical centra are opisthoceolous with dorsally arched
799 ventral surface. In remnant elements of the cervical series the anterior articular surface becomes
800 flat or slightly convex, and their corresponding posterior articular surface becomes less concave,
801 resulting the platycoelous centra. The centra of the postaxial cervicals are anteroposteriorly longer
802 than dorsoventrally high, whereas the length/height ratio gradually decreases posteriorly through
803 the cervical series. A distinct rim (Fig. 13 A-C) is present on the anterior articular surface of the
804 anterior cervicals, and it is especially well defined on the third cervical. This distinct rim also
805 occurs on anterior cervicals of *Yunyangosaurus* (Dai et al., 2020), whereas all the postaxial
806 cervical vertebrae bear such rim in *Torvosaurus* (Britt, 1991). In all postaxial cervicals, the anterior
807 and posterior articular surfaces are slightly wider than high.

808 The lateral surface of each of the postaxial cervical centra is excavated by a single pleurocoel,
809 which is positioned posterodorsal to the parapophysis. In the third cervical (Fig. 13 A) the
810 pleurocoel deeply invades the lateral surface of the centrum, leading to a very transversely narrow
811 ventral surface (Fig. 14 C) of central part. But this narrowing ventral surface does not run through
812 the whole length of centrum to form a ventral keel. The ventral surfaces of following cervical
813 vertebrae become broad and flat and by the 10th cervical vertebra the ventral keel appears with a

814 ventrally vaulted process anterior to it. In the fourth and fifth cervical, the pleurocoel is leading to
815 the neural canal. In the eighth and ninth cervical the pleurocoel is anteroposteriorly elongated and
816 dorsally roofed by a thin lamina.

817 The diapophysis of each postaxial cervical is lateroventrally extended, and bears a smooth articular
818 surface with ellipse profile. The parapophysis is positioned ventral to the mid-height of the centrum
819 and adjacent to the anterior articular surface in each cervical. In the third and the last two cervicals
820 the parapophysis is strongly shortened and ended with oval-shaped surface, whereas it protrudes
821 lateroventrally in other cervicals. The laterally elongated parapophyses in medial cervicals also
822 occur in *Neovenator* (Brusatte et al., 2008). In the last cervical the parapophysis is followed by a
823 prominent ridge, which marks the bottom of the pleurocoel and shallows posteriorly.

824 The prezygopophysis projects anteriorly from the base of diapophysis, and is connected with the
825 diapophysis laterally through the prezygodiapophyseal lamina (prdl). The paired prezygopophyses
826 are well separated dorsolateral to the neural arch, and are medially connected by the
827 intraprezygopophyseal lamina (tprl). The prezygopophysis has a sub-ellipse shaped and smooth
828 articular facet, which faces anterodorsally and medially. The spinoprezygopophyseal lamina (sprl)
829 laterally demarcates this facet, and connect the prezygopophysis with the neural spine. Throughout
830 the whole cervical series this facet turns more anteromedially, and the anteroposterior distance
831 between pre- and postzygopophysis gradually shortens. The posterodorsally and laterally projected
832 postzygopophysis is more strongly developed than the prezygopophysis, with lateroventrally and
833 posteriorly faced articular surface. In the last three cervicals (Fig. 13 F-H), the postzygopophyseal
834 facets turn to face more posteriorly than that of the preceding elements in the series. The
835 postzygodiapophyseal lamina (podl) runs from the base of the diapophysis posteriorly to the distal
836 end of the postzygopophysis or epipophysis. The spinopostzygopophyseal lamina (spol) originates
837 posteriorly from the base of the neural spine and ends at the distal end of the articular surface of
838 the postzygopophysis. Only the first three postaxial cervicals have well developed epipophysis,
839 which emerges posterolaterally and dorsally to the postzygopophysis. In fourth and fifth cervical
840 the epipophysis is extended well beyond the posterior margin of the postzygopophysis and forms
841 a dorsoventrally thin plate-like structure.

842 In the third and fourth cervical (Fig. 13 A, B), the anterior rim of the neural spine bears an
843 anterodorsal oriented process, resulting the concave lateral profile above and below this process.
844 Such process positioned at the anterodorsal rim of the anterior cervicals also occurs in
845 *Acrocanthosaurus* (Harris, 1998), but in which this process protrudes more anteriorly and past the
846 base of neural spine. The posterior rim of the neural spine of these two elements is posterodorsally
847 convex, thus the posteriormost point is situated at nearly midheight. In subsequent cervicals the
848 neural spine increases in height gradually, and is dorsoventrally higher than anteroposteriorly long
849 since the sixth cervical. In the eighth, ninth and tenth cervicals (Fig. 13 F-H) the neural spine is

850 prominently dorsally elongated, with the distal end fanning out anteroposteriorly in lateral view.
851 Whereas in derived metriacanthosaurids (*Dong et al., 1983; Currie & Zhao, 1993; Gao, 1992,*
852 *1999*), neural spines in posterior cervical vertebrae are slender and rod-like, this condition might
853 provide more spaces for upward mobility of the neck. In ninth (Fig. 14 G-I) and 10th cervicals, a
854 shallow groove runs dorsoventrally along the anterior and posterior rims of the neural spine.

855 Several bony laminae connect the neural arch and the centrum and separate the space between
856 them into several pneumatic chambers as in most Theropods. In the first five postaxial cervicals
857 the anterior centrodiaepophyseal lamina (acdl) and centraprezygopophyseal lamina (cprl) are not
858 very developed and laterally obscured by the ventrally oriented diapophyses. Due to the short
859 distance between the neural arch and centrum in anterior cervicals, the centrapostzygopophyseal
860 laminae of these elements are poorly-developed. In the rest of the cervical series the distance
861 between the arch and centrum increases with the elevation of the diapophysis from the
862 parapophysis, resulting that aforementioned three bony laminae become more prominent. In the
863 first three postaxial cervicals the postzygodiapophyseal laminae (podl) do not continue onto the
864 pedicle of the diapophyses. In the third cervical this lamina is especially weak-developed and even
865 discontinuous to the base of the postzygopophysis. In the last three cervicals, a pneumatic fossa
866 excavates anteriorly into the ventral surface of the postzygodiapophyseal lamina (podl), as in
867 *Sinraptor (Currie & Zhao, 1993)*. All postaxial cervicals bear notable prezygodiapophyseal
868 laminae (prdl) and posterior centradiaepophyseal laminae (pcdl).

869 The first dorsal vertebra (Fig. 13 I) is platycoelous, with a flat anterior articular surface and a
870 slightly concave posterior articular surface. The anterior and posterior articular surface are slightly
871 wider than high as in cervical vertebrae. The neural arch and the centrum of the first dorsal vertebra
872 are in further distance compared to those in the cervical vertebrae. This extension is followed by
873 the more elongated bony laminae connecting the neural arch and the centrum. The diapophysis is
874 more laterally and horizontally oriented instead of pointing ventrolaterally. The parapophysis does
875 not protrude laterally and its articular surface is immediately lateral to the anterior articular surface
876 of the centrum and subtriangular in shape. The pre- and postzygopophysis decreases in height,
877 followed by the reduction of inclination of the pre- and postzygodiapophyseal lamina in lateral
878 view. The neural spine is approximately 1.5 times as dorsoventrally high as anteroposteriorly long,
879 with a sub-rectangular lateral profile. The groove running along the anterior rim of the neural spine
880 excavates deeper than those of former cervical vertebrae. As in postaxial cervicals, a single
881 pleurocoel penetrates either side of the centrum, but these pelurocoels on both left and right side
882 are straightly connected without any bony walls. The ventral part of the centrum is similar to that
883 of the last cervical vertebra, with a ridge originated from the posterior end of the parapophysis
884 forming the lateral floor of the peurocoel, and a developed ventral keel running through the
885 centrum.

886

887 **Phylogenetic analysis**

888 The phylogenetic analysis resulted in 1152 MPTs, with each MPTs having a length of 1290 steps
889 (CI = 0.364, RI = 0.660). The strict consensus tree (Fig. 14) places *Yuanmouraptor* at the most
890 'basal' position in the Metriacanthosauridae, forming a polytomy with *Xuanhanosaurus* and a
891 monophyletic group defined by *Yangchuanosaurus* and *Sinraptor*. The Metriacanthosauridae in
892 our analysis is supported by seven unambiguous synapomorphies: squamosal forms a flange
893 covering quadrate head laterally (character 87-1); acute angle between the occipital condyle and
894 the basal tubera (character 123-1); external mandibular fenestra is 15% longer than the total
895 mandible length (character 133-1); dorsoventral depth of surangular above external mandibular
896 fenestra less than half of the height of mandible (character 134-0); well-developed and broad
897 spinopostzygopophyseal lamina (character 183-0); manus shorter than arm plus forearm (character
898 268-0); presence of metacarpal IV but lack of IV phalanges and whole digit V (character 269-0).
899 Furthermore, three major lineages of basally branching tetanurans (Megalosauroidae,
900 Coelurosauria, and Allosauroidae) are supported by this phylogenetic analysis, and recovered a
901 Carnosauria in which Piatnitzkysauridae forms the sister-group to Avetheropoda (Allosauroidae +
902 Coelurosauria).

903

904 **DISCUSSION**

905 **Comparison with Jurassic Metriacanthosauridae in China and morphology** 906 **transition within Metriacanthosauridae lineage**

907 As shown in the result of our phylogenetic analysis, the metriacanthosaurids excluding
908 *Xuanhanosaurus* (Dong, 1984) and *Yuanmouraptor* formed two lineages together to form a
909 monophyletic clade within Metriacanthosauridae. In other words, *Yuanmouraptor*,
910 *Xuanhanosaurus*, and the clade formed a basal trichotomy within Metriacanthosauridae.

911 The Middle Jurassic *Xuanhanosaurus* (Dong, 1984) was considered to fall within
912 Megalosauroidae or in close relationship with Piatnitzkysauridae in previous studies (Benson,
913 2010; Rauhut et al., 2016; Rauhut & Pol, 2019; Dai et al., 2020). In our phylogenetic analysis,
914 *Xuanhanosaurus* was recovered as a member of Metriacanthosauridae, as in Carrano et al. (2012),
915 but this placement is poorly supported with only two characters: relatively short manus and
916 developed metacarpal IV with lack of IV phalanges and digit V, shared with CNM V214 (Dong et
917 al., 1983) and '*Szechuanosaurus*' *zigongensis* (Gao, 1993) respectively. Therefore, the
918 phylogenetic position of *Xuanhanosaurus* still needs to be testified by a detailed study of the taxon
919 in the future. The overlapping materials of *Xuanhanosaurus* with *Yuanmouraptor* are limited to
920 two posterior cervical vertebrae. The eighth cervical centrum of *Xuanhanosaurus* is evidently

921 opisthocoelous, in contrast with the platycoelous condition in that of *Yuanmouraptor*. Due to the
922 uncertain phylogenetic position of *Xuanhanosaurus*, *Yuanmouraptor* is considered as the most basal
923 representative of Metriacanthosauridae.

924 *Sinraptor dongi* (Currie & Zhao, 1993), *S. hepingensis* (Gao, 1992, 1999), and *Yangchuanosaurus*
925 *shangyouensis* (Dong et al., 1978, 1983) represent derived members in Metriacanthosauridae and
926 all lived in Late Jurassic. Materials of these taxa reach a high degree of completeness, and provide
927 significant taxonomic information. These three taxa are large-sized theropods, and the skull length
928 could reach approximately two times the condition in *Yuanmouraptor*. In *S. dongi*, *S. hepingensis*,
929 and *Y. shangyouensis*, the skull and vertebrae are highly pneumatized, such as the pneumatic
930 foramen on the lateral surface of the jugal and perforated pleurocoels on the axial centrum.
931 Whereas in *Yuanmouraptor* the jugal and axial centrum are not pneumatized. The ventral process
932 of the postorbital of three derived metriacanthosaurids has a small suborbital flange, which might
933 mark the ventral limit of the eyeball, whereas in *Yuanmouraptor* the ventral process of the
934 postorbital is smooth and slightly concave below the eyeball. All three derived metriacanthosaurids
935 bear rugose ornaments on the upper part of the skull, such as heavy rugosity on the nasal, well-
936 developed lacrimal horn, and large rugose boss forming the anterior process of the postorbital.
937 Though the nasal of *Yuanmouraptor* was not preserved, the lacrimal and postorbital only possess
938 slight rugosity. The cervical vertebrae of derived metriacanthosaurids are strongly opisthocoelous
939 with ball and socket articular surface, and the axial intercentrum is anterodorsally flexed. This
940 condition shows greater mobility than that of *Yuanmouraptor*, in which the cervical vertebrae are
941 platycoelous and the ventral surface of the axial intercentrum is continuous with that of the
942 centrum. The anteroposteriorly narrow neural spines in posterior cervical vertebrae also indicate a
943 more upward flexible neck in derived metriacanthosaurids. By contrast, the sheet-like neural
944 spines of posterior cervical vertebrae in *Yuanmouraptor* might limit the upward flexibility of the
945 neck.

946 Within the monophyletic clade excluding *Yuanmouraptor* and *Xuanhanosaurus* in the
947 Metriacanthosauridae, one lineage leads to *Yangchuanosaurus* (Dong et al., 1978, 1983), and
948 another lineage is represented by *Sinraptor* (Gao, 1992; Currie & Zhao, 1993). The clade
949 comprising the members of the latter lineage was named as Metriacanthosaurinae by Carrano et
950 al. (2012). These two lineages are distinct in many aspects. In the axial skeleton, the anterior dorsal
951 vertebrae of Metriacanthosaurinae have prominent ventral keel, whereas in another lineage the
952 keel is weakly developed. In the pelvic girdle, the angle between the long axis of pubis and pubic
953 boot is less than 60° in Metriacanthosaurinae, distinguished from the nearly perpendicular boot
954 and shaft of the pubis in *Yangchuanosaurus* lineage. In Metriacanthosaurinae the ischial shaft is
955 ventrally curved and the distal end is slightly expanded, which differs from that the ischial shaft is
956 straight and the distal end of ischium is notably expanded to form an ischial boot in

957 *Yangchuanosaurus* lineage. Whereas the distal end of the ischium of *Yangchuanosaurs*
958 *shangyouensis* is slightly expended and similar to the condition in Metriacanthosaurinae, might
959 suggesting that this trait is gained independently in these taxa. In the hindlimbs, members of
960 Metriacanthosaurinae possess bulbous fibular crest on the tibia, in contrast to the narrow and
961 lamina-like fibular crest of the tibia in *Yangchuanosaurus* lineage.

962 *Shidaisaurus* (Wu et al., 2009) was found in Chuanjie Formation (Middle Jurassic) in Lufeng City,
963 Yunnan, which is 85 km from the type locality of *Yuanmouraptor*. *Shidaisaurus* was the first
964 tetanuran reported in Yunnan Province. The skull roof, dorsal part of the occiput, and axis of
965 *Shidaisaurus* are preserved, and these elements could be compared with *Yuanmouraptor*. Both
966 *Yuanmouraptor* and *Shidaisaurus* possess paired frontals broader than long, which generally occur
967 in Allosauroidea; however, in Megalosauroidea and more basal theropods, the paired frontals are
968 anteroposteriorly longer than transversely wide. Similar to *Shidaisaurus*, a slight margin of the
969 frontal contributes to the dorsal margin of the orbit in *Yuanmouraptor*, this also occurs in *Sinraptor*
970 *dongi* (Currie & Zhao, 1993). The supratemporal fossa of *Shidaisaurus* is bounded by abruptly
971 elevated surfaces of the frontals and parietal, which form a very clear border of the supratemporal
972 fossa, this is similar to the condition in *Sinraptor dongi* (Currie & Zhao, 1993). Whereas in
973 *Yuanmouraptor*, the border of the supratemporal fenestra does not have well-defined boundary,
974 and the surfaces of the surrounding frontals and parietal are plain and gently sloped. The occiput
975 of *Shidaisaurus* and *Yuanmouraptor* share a similar posteroventrally directed paroccipital process,
976 with the ventral base of which located beneath the occipital condyle, a condition generally
977 developed in Allosauroidea. However, the supraoccipital of *Yuanmouraptor* forms a moderate part
978 of the dorsal rim of the foramen magnum, differing from *Shidaisaurus* in which the supraoccipital
979 does not contribute to form the dorsal margin of the foramen magnum. An atlas-axis complex is
980 the only preserved cervical element of *Shidaisaurus*. The axial centrum of *Shidaisaurus* bears
981 some similarities to that of *Yuanmouraptor*, including broad spinopostzygapophyseal lamina and
982 absence of pleurocoels. The axial intercentrum of *Shidaisaurus* has an anterodorsal inclined ventral
983 surface, followed by an anterodorsally faced anterior articular surface, which resembles the
984 condition in derived metriacanthosaurid *Yangchuanosaurus* (Dong et al., 1983) and *Sinraptor*
985 (Currie & Zhao, 1993). However, the alignment of the atlas-axis complex is different in
986 *Yuanmouraptor*, in which the ventral surface of the axial intercentrum is parallel with the axial
987 centrum, but the anterior articular surface of the axial intercentrum also faces anterodorsally,
988 resulting in a triangular lateral profile of the axial intercentrum. This indicates that *Yuanmouraptor*
989 could also bring the neck underneath the occipital condyle more or less to support the skull as more
990 derived Late Jurassic metriacanthosaurids, and might represent an early stage of the arrangement of
991 the atlas-axis complex during the evolution of Metriacanthosauridae. Although *Yuanmouraptor*
992 and *Shidaisaurus* share similar geological distribution and approximately contemporaneous

993 stratigraphic unit which were known as Middle Jurassic (Huang et al., 2005; Fang et al., 2008),
994 the difference in morphology along with the support of our phylogenetic analysis shows the
995 validity of *Yuanmouraptor jinshajiangensis* gen. et sp. nov.

996 The Late Jurassic CNM V214 (Dong et al., 1983) and the Middle Jurassic '*Szechuanosaurus*'
997 *zigongensis* (Gao, 1992) are also positioned as derived metriacanthosaurids by the phylogenetic
998 analysis and form a monophyletic group with *Sinraptor dongi* (Currie & Zhao, 1993), *Sinraptor*
999 *hepingensis* (Gao, 1992), and *Yangchuanosaurus* (Dong et al., 1978, 1983). The first reports of
1000 CNM V214 and '*S.*' *zigongensis* regarded them as the neotype of '*Szechuanosaurus*' *campi*
1001 (Young, 1942) and a new species of the genus '*Szechuanosaurus*' respectively. The type species
1002 of genus '*Szechuanosaurus*', '*S. campi*', was based on four isolated teeth, and was considered as
1003 invalid (Wu et al., 2009; Carrano et al., 2012). Due to the lack of detailed restudies and
1004 phylogenetic analyses of these two specimens for decades, CNM V214 and '*S.*' *zigongensis* have
1005 not been given the formal taxonomic names so far. The information about CNM V214 is very
1006 limited, with part of the cervical series overlapping with *Yuanmouraptor*. The axial complex of
1007 CNM V214 is similar to that of *S.dongi*, *S. hepingensis*, and *Yangchuanosaurus*, with the
1008 anterodorsally tilted ventral surface of the intercentrum and well-developed pleurocoels on the
1009 centrum. The maxilla of '*S.*' *zigongensis* is similar to that of *Yuanmouraptor*, with well-developed
1010 antorbital fossa. However, the morphology of the posterior cervical vertebrae of '*S.*' *zigongensis*
1011 resembles the condition in those Late Jurassic forms, in which the neural spines are
1012 anteroposteriorly narrow and rod-like.

1013 Many character transitions occurred during the evolution of Metriacanthosauridae from the Middle
1014 Jurassic to the Late Jurassic. First, as shown in *Yuanmouraptor*, the basal-branching Middle
1015 Jurassic members of this clade do not possess a well-developed pneumatic system as in those Late
1016 Jurassic descendants, such as the lack of pneumatic foramen on jugal and pleurocoels on axial
1017 centrum. The latter condition also occurs in basal-branching metriacanthosaurid *Shidaisaurus* (Wu
1018 et al., 2009). Second, the ornamentations of the skull have been changed from a slight rugose brow
1019 in *Yuanmouraptor* to a prominent lacrimal horn and heavy rugosity on postorbital in *Sinraptor*
1020 (Gao, 1992; Currie & Zhao, 1993) and *Yangchuanosaurus* (Dong et al., 1983). Third, the
1021 alignment of the atlas-axis complex and morphology of cervical vertebrae have been changed to
1022 improve the mobility of the neck. In the primitive stage, as shown in *Yuanmouraptor*, the ventral
1023 surface of the axial intercentrum and centrum are continuous, and subsequent cervical vertebrae
1024 are platycoelous. This condition has been changed to that the ventral surface of axial intercentrum
1025 is notably inclined anterodorsally to bring the neck underneath the skull and cervical vertebrae are
1026 strongly opisthocoelous with ball-and-socket articular surface in *Yangchuanosaurus* and
1027 *Sinraptor*. Furthermore, to increase the upward flexibility of the posterior part of the neck, the
1028 neural spines of posterior cervical vertebrae altered from sheet-like in *Yuanmouraptor* to rod-like

1029 in those Late Jurassic descendants. Two Middle Jurassic taxa, *Shidaisaurus* and
1030 '*Szechuanosaurus*' *zigongensis* (Gao, 1993) could be regarded as transitional forms. In
1031 '*Szechuanosaurus*' *zigongensis* (Gao, 1993), the neural spines of posterior cervical vertebrae are
1032 also anteroposteriorly constricted and nearly rod-like, but the articular surfaces of cervical centra
1033 are platycoelous. *Shidaisaurus* possesses anterodorsally inclined axial intercentrum, but lacks
1034 pleurocoels on the axial centrum.

1035

1036 **Implications on phylogeny of basal-branching tetanurans**

1037 Since three major lineages (Megalosauroidae, Allosauroidae, and Coelurosauria) within Tetanurae
1038 were proposed by Carrano *et al.* (2012), alternative opinions (Rauhut & Pol, 2019; Lamanna *et*
1039 *al.*, 2020; Schade *et al.*, 2023; Rauhut *et al.*, 2024) upon the interrelationship of tetanurans were
1040 put forward in past decade. Although the result recovered by our phylogenetic analysis approaches
1041 to the three-major-clade pattern within Tetanurae, this topology of diverging is unstable with
1042 relatively low scores of Bremer support in many nodes (see the online Supplemental File S2 for
1043 details). Among the nodes within Tetanurae, Spinosauridae and Coelurosauria (with the exception
1044 of *Lourinhanosaurus*) are well-supported, with Bremer support scored 3. Besides, Allosauria
1045 (Allosauridae + Carcharodontosauria), and Metriacanthosaurinae (Carrano *et al.*, 2012) are less
1046 well supported with Bremer support scored 2. However, the placement of Piatnitzkysauridae
1047 within the Allosauroidae is rather stable, with three additional steps needed to recover its affinity
1048 to Megalosauroidae. The low Bremer support of many nodes within Tetanurae might suggest that
1049 independent acquisitions of characters occurred multiple times during Early and Middle Jurassic.
1050 At least eight taxa from western China are located near the node Allosauroidae by our phylogenetic
1051 analysis, but taxa of other clades of basal tetanurans in this region are scarce, this is probably due
1052 to the artificial effects rather than the reflection of real proportion of different clades within basal-
1053 branching tetanurans. The finding of *Yuanmouraptor* provides an example of early stage in
1054 tetanuran evolution. Many characters present in *Yuanmouraptor* are shared with megalosaurid
1055 theropods or non-tetanuran theropods, indicating that high level of similarities among these Early
1056 and Middle Jurassic theropods. Thus, findings of key taxa to bridge the gap between non-tetanuran
1057 ancestors and a variety of derived tetanuran clades are important to testify whether similar
1058 character states in different clades are the result of homology or homoplasy. Meanwhile, the
1059 construction and sampling of characters, accuracy of state scores, and issues of sampling are also
1060 strongly related to alleviate phylogenetic uncertainty (Lovegrove *et al.*, 2024). The review and
1061 redescription of the named taxa are of great significance. There are still many taxa (Dong *et al.*,
1062 1978; He, 1984; Dong *et al.*, 1983; Dong & Tang, 1985; Gao, 1992, 1993, 1999; Li *et al.*, 2009)
1063 reported in China lacking detailed osteological descriptions. New anatomic information helping to
1064 resolve the phylogenetic problems will be extracted after the detailed re-examination and

1065 description of those taxa in future works.

1066

1067 CONCLUSIONS

1068 A new metriacanthosaurid, *Yuanmouraptor jinshajiangensis* gen. et sp. nov, is established based
1069 on a relatively complete skull, a complete cervical series, and an anterior-most dorsal vertebra.
1070 *Yuanmouraptor* is diagnosed by a unique combination of characters, especially six
1071 autapomorphies. Phylogenetic analysis placed *Yuanmouraptor* at a basal-branching position
1072 within Metriacanthosauridae. Although the type locality and living age of *Yuanmouraptor*
1073 resemble those of *Shidaisaurus*, many characters manifest that these two are different taxa.
1074 *Yuanmouraptor* presents the most complete craniums among basal-branching tetanurans reported
1075 in Middle Jurassic China, and provides valuable information concerning the morphology transition
1076 of cranium and cervical vertebrae during the cause of metriacanthosaurid evolution. In addition,
1077 our phylogenetic analysis recovered that the phylogenetic position of Piatnitzkysauridae is more
1078 closed to Allosauroidea than to Megalosauroidea, and three major lineages within Tetanurae are
1079 supported. However, due to the lack of consensus upon the phylogenetic relationship within basal-
1080 branching tetanurans over past decades, more accuracy in character coding and new findings of
1081 early members of this clade are needed to testify this new alternative phylogenetic topology.

1082 INSTITUTIONAL ABBREVIATIONS

1083 CNM Chongqing Natural History Museum;

1084 LFGT The Bureau of Natural Resources of Lufeng City, Yunnan, China.

1085

1086 Acknowledgements

1087 This research greatly benefited from discussions with Qian-Nan Zhang, Ya-Ming Wang, Yan-
1088 Chao Wang, and Jian Yi. This research was supported by the National Natural Science Foundation
1089 of China (42288201, 42372030, and 42002014), the Beijing Natural Science Foundation
1090 (5224037) and Expert Local Level Scientific Workstation of Yunnan Province.

1091

1092 References

- 1093 Allain R. 2002. Discovery of megalosaur (Dinosauria, Theropoda) in the middle Bathonian of Normandy (France)
1094 and its implications for the phylogeny of basal Tetanurae. *Journal of Vertebrate Paleontology* **22**(3):548-
1095 563. DOI 10.1671/0272-4634(2002)022[0548:Domdti]2.0.Co;2
- 1096 Barker CT, Hone DWE, Naish D, Cau A, Lockwood JAF, Foster B, Clarkin CE, Schneider P, Gostling NJ.
1097 2021. New spinosaurids from the Wessex Formation (Early Cretaceous, UK) and the European origins of
1098 Spinosauridae. *Scientific Reports* **11**(19340):1-15. DOI 10.1038/s41598-021-97870-8

- 1099 **Barker CT, Naish D, Newham E, Katsamenis OL, Dyke G. 2017.** Complex neuroanatomy in the rostrum of the
1100 Isle of Wight theropod *Neovenator salerii*. *Scientific Reports* **7(1)**:3749. DOI 10.1038/s41598-017-03671-3
- 1101 **Benson RBJ. 2008.** A redescription of '*Megalosaurus hesperis* (Dinosauria, Theropoda) from the Inferior Oolite
1102 (Bajocian, Middle Jurassic) of Dorset, United Kingdom. *Zootaxa* **1931**:57-67. DOI 10.5281/zenodo.184841
- 1103 **Benson RBJ. 2010.** A description of *Megalosaurus bucklandii* (Dinosauria: Theropoda) from the Bathonian of the
1104 UK and the relationships of Middle Jurassic theropods. *Zoological Journal of the Linnean Society*
1105 **158(4)**:882-935. DOI 10.1111/j.1096-3642.2009.00569.x
- 1106 **Bonaparte JF. 1986.** Les Dinosauriens (Carnosauriens, Allosauridés, Sauropodes, Cetiosauridés) du Jurassique Moyen
1107 de Cerro Cóndor (Chubut, Argentine). *Annales de Paléontologie* **72**:247-289.
- 1108 **Britt BB. 1991.** The theropods of the Dry Mesa Quarry (Morrison Formation), Colorado: with emphasis on the
1109 osteology of *Torvosaurus tanneri*. *Brigham Young University, Geology Studies* **37**:1-72.
- 1110 **Brusatte SL, Benson RBJ, Currie PJ, Zhao XJ. 2010a.** The skull of *Monolophosaurus jiangi* (Dinosauria:
1111 Theropoda) and its implications for early theropod phylogeny and evolution. *Zoological Journal of the*
1112 *Linnean Society* **158(3)**:573-607. DOI 10.1111/j.1096-3642.2009.00563.x
- 1113 **Brusatte SL, Benson RBJ, Hutt S. 2008.** *The osteology of Neovenator salerii (Dinosauria: Theropoda) from the*
1114 *Wealden Group (Barremian) of the Isle of Wight*: Monograph of the Palaeontographical Society.
- 1115 **Brusatte SL, Carr TD, Erickson GM, Bever GS, Norell MA. 2009.** A long-snouted, multihorned tyrannosaurid
1116 from the Late Cretaceous of Mongolia. *Proceedings of the National Academy of Sciences* **106(41)**:17261-
1117 17266. DOI 10.1073/pnas.0906911106
- 1118 **Brusatte SL, Chure DJ, Benson RBJ, Xu X. 2010b.** The osteology of *Shaochilong maortuensis*, a
1119 carcharodontosaurid (Dinosauria: Theropoda) from the Late Cretaceous of Asia. *Zootaxa* **2334(1)**:1-46. DOI
1120 10.5281/zenodo.193148
- 1121 **Brusatte SL, Sereno PC. 2007.** A new species of *Carcharodontosaurus* (Dinosauria: Theropoda) from the
1122 Cenomanian of Niger and a revision of the genus. *Journal of Vertebrate Paleontology* **27(4)**:902-916. DOI
1123 10.1671/0272-4634(2007)27[902:ANSOCD]2.0.CO;2
- 1124 **Brusatte SL, Sereno PC. 2008.** Phylogeny of Allosauroidea (Dinosauria: Theropoda): Comparative analysis and
1125 resolution. *Journal of Systematic Palaeontology* **6(2)**:155-182. DOI 10.1017/s1477201907002404
- 1126 **Buffetaut E, Suteethorn V, Tong H. 1996.** The earliest known tyrannosaur from the Lower Cretaceous of Thailand.
1127 *Nature* **381(6584)**:689-691. DOI 10.1038/381689a0
- 1128 **Carr TD, Varricchio DJ, Sedlmayr JC, Roberts EM, Moore JR. 2017.** A new tyrannosaur with evidence for
1129 anagenesis and crocodile-like facial sensory system. *Scientific Reports* **7(1)**:44942. DOI 10.1038/srep44942
- 1130 **Carrano MT, Benson RBJ, Sampson SD. 2012.** The phylogeny of Tetanurae (Dinosauria: Theropoda). *Journal of*
1131 *Systematic Palaeontology* **10(2)**:211-300. DOI 10.1080/14772019.2011.630927
- 1132 **Carrano MT, Loewen MA, Sertich JWJ. 2011.** *New materials of Masiakasaurus knopfleri Sampson, Carrano, and*
1133 *Forster, 2001, and Implications for the Morphology of the Noasauridae (Theropoda: Ceratosauria)*:
1134 Smithsonian Institution Scholarly Press.
- 1135 **Choiniere JN, Clark JM, Forster CA, Xu X. 2010.** A basal coelurosaur (Dinosauria: Theropoda) from the Late
1136 Jurassic (Oxfordian) of the Shishugou Formation in Wucuiwan, People's Republic of China. *Journal of*
1137 *Vertebrate Paleontology* **30(6)**:1773-1796. DOI 10.1080/02724634.2010.520779
- 1138 **Colbert EH. 1989.** *The Triassic dinosaur Coelophysis*. Arizona: Museum of Northern Arizona Press.
- 1139 **Coria RA, Currie PJ. 2002.** The braincase of *Giganotosaurus carolinii* (Dinosauria: Theropoda) from the Upper

- 1140 Cretaceous of Argentina. *Journal of Vertebrate Paleontology* **22(4)**:802-811. DOI 10.1671/0272-
1141 4634(2002)022[0802:Tbogcd]2.0.Co;2
- 1142 **Coria RA, Currie PJ. 2006.** A new carcharodontosaurid (Dinosauria, Theropoda) from the Upper Cretaceous of
1143 Argentina. *Geodiversitas* **28(1)**:71-118.
- 1144 **Coria RA, Currie PJ. 2016.** A New Megaraptoran Dinosaur (Dinosauria, Theropoda, Megaraptoridae) from the Late
1145 Cretaceous of Patagonia. *PLoS One* **11(7)**:e0157973. DOI 10.1371/journal.pone.0157973
- 1146 **Coria RA, Salgado L. 1995.** A new giant carnivorous dinosaur from the Cretaceous of Patagonia. *Nature* **337**:224-
1147 226. DOI 10.1038/377224a0
- 1148 **Cullen TM, Larson DW, Witton MP, Scott D, Maho T, Brink KS, Evans DC, Reisz R. 2023.** Theropod dinosaur
1149 facial reconstruction and the importance of soft tissues in paleobiology. *Science* **379(6639)**:1348-1352. DOI
1150 10.1126/science.abo7877
- 1151 **Currie PJ, Carpenter K. 2000.** A new specimen of *Acrocanthosaurus atokensis* (Theropoda, Dinosauria) from the
1152 Lower Cretaceous Antlers Formation (Lower Cretaceous, Aptian) of Oklahoma, USA. *Geodiversitas*
1153 **22(2)**:207-246.
- 1154 **Currie PJ, Zhao XJ. 1993.** A new carnosaur (Dinosauria, Theropoda) from the Jurassic of Xinjiang, People's
1155 Republic of China. *Canadian Journal of Earth Sciences* **30(10)**:2037-2081. DOI 10.1139/e93-179
- 1156 **Dai H, Benson R, Hu XF, Ma QY, Tan C, Li N, Xiao M, Hu HQ, Zhou YX, Wei ZY, Zhang F, Jiang S, Li DQ,
1157 Peng GZ, Yu YL, Xu X. 2020.** A new possible megalosauroid theropod from the Middle Jurassic Xintiangou
1158 Formation of Chongqing, People's Republic of China and its implication for early tetanuran evolution. *Sci
1159 Rep* **10(1)**:139. DOI 10.1038/s41598-019-56959-x
- 1160 **Dong ZM. 1984.** A new Theropod dinosaur from the middle Jurassic of Sichuan Basin. *Vertebrata Palasiatica*
1161 **22(3)**:213-218.
- 1162 **Dong ZM, Tang ZL. 1985.** A new Mid-Jurassic theropod (*Gasosaurus constructus* gen et sp. nov.) from Dashanpu,
1163 Zigong, Sichuan Province, China. *Vertebrata Palasiatica* **23(1)**:77-83.
- 1164 **Dong ZM, Zhang YH, Li XM, Zhou SW. 1978.** A new carnosaur from Yongchuan County, Sichuan Province.
1165 *Chinese Science Bulletin* **23(5)**:302-304.
- 1166 **Dong ZM, Zhou SW, Zhang YH. 1983.** Dinosaurs from the Jurassic of Sichuan. *Palaeontologica Sinica* **162C(23)**:1-
1167 136.
- 1168 **Eddy DR, Clarke JA. 2011.** New information on the cranial anatomy of *Acrocanthosaurus atokensis* and its
1169 implications for the phylogeny of Allosauroida (Dinosauria: Theropoda). *PLoS One* **6(3)**:e17932. DOI
1170 10.1371/journal.pone.0017932
- 1171 **Fang XS, Li PX, Zhang ZJ, Cheng ZW, Pang QQ, Zhang ZW, Huang BC. 2008.** *The Jurassic Red Bed in the
1172 Cental Yunan of China*. Peijing: Geology Press.
- 1173 **Gao YH. 1992.** *Yangchuanosaurus hepingensis*-a new species of carnosaur from Zigong, Sichuan. *Vertebrata
1174 Palasiatica* **30(4)**:313-324.
- 1175 **Gao YH. 1993.** A new species of *Szechuanosaurus* from the middle Jurassic of Dshanpu, Zigong, Sichuan. *Vertebrata
1176 Palasiatica* **31(4)**:308-314.
- 1177 **Gao YH. 1999.** *A complete Carnosaur skeleton from Zigong, Sichuan: Yangchunosaurus hepingensis*: Sichuan
1178 Scientific & Technological Press.
- 1179 **Gauthier J. 1986.** Saurischian monophyly and the origin of birds. *Memoirs of the California Academy of Science* **8**:1-
1180 55.

- 1181 **Goloboff PA, Morales ME. 2023.** TNT version 1.6, with a graphical interface for MacOS and Linux, including new
1182 routines in parallel. *Cladistics* **39(2)**:144-153. DOI 10.1111/cla.12524
- 1183 **Harris JD. 1998.** *A reanalysis of Acrocanthosaurus atokensis, its phylogenetic status, and paleobiogeographic*
1184 *implications, based on a new specimen from Texas*: New Mexico Museum of Natural History.
- 1185 **He XL. 1984.** *The Vertebrate Fossils of Sichuan*. Chengdu: Sichuan Scientific and Technological Publishing House.
- 1186 **Hendrickx C, Hartman SA, Mateus O. 2015.** An overview of non-avian theropod discoveries and classification.
1187 *PalArch's Journal of Vertebrate Palaeontology* **12(1)**:1-73.
- 1188 **Hendrickx C, Mateus O. 2014.** *Torvosaurus gurneyi* n. sp., the Largest Terrestrial Predator from Europe, and a
1189 Proposed Terminology of the Maxilla Anatomy in Nonavian Theropods. *PLoS One* **9(3)**:1-25. DOI
1190 10.1371/journal.pone.0088905
- 1191 **Holtz TRJ, Molnar RE, Currie PJ. 2004.** Basal Tetanurae. In: Weishampel DB, Dodson P, Osmólska H, eds. *The*
1192 *Dinosauria Second edition*: University of California Press, Berkeley., 71-110.
- 1193 **Huang BC. 2005.** Magnetostratigraphy of the Jurassic in Lufeng, central Yunnan. *Geological Bulletin of China*
1194 **24(4)**:322-328.
- 1195 **Huene FV. 1923.** Carnivorous Saurischia in Europe Since the Triassic. *Geological Society of America Bulletin*
1196 **34(3)**:449-458. DOI 10.1130/gsab-34-449
- 1197 **Lamanna MC, Casal GA, Martínez RDF, Ibiricu LM. 2020.** Megaraptorid (Theropoda: Tetanurae) Partial
1198 Skeletons from the Upper Cretaceous Bajo Barreal Formation of Central Patagonia, Argentina: Implications
1199 for the Evolution of Large Body Size in Gondwanan Megaraptorans. *Annals of Carnegie Museum* **86(3)**:255-
1200 294. DOI 10.2992/007.086.0302
- 1201 **Li F, Peng GZ, Ye Y, Jiang S, Huang DX. 2009.** A new carnosaur from the Late Jurassic of Qianwei, Sichuan,
1202 China. *Acta Geologica Sinica* **83(9)**:1203-1213.
- 1203 **Lovegrove J, Upchurch P, Barrett PM. 2024.** Untangling the tree or unravelling the consensus? Recent
1204 developments in the quest to resolve the broad-scale relationships within Dinosauria. *Journal of Systematic*
1205 *Palaeontology* **22(1)**:234533. DOI 10.1080/14772019.2024.2345333
- 1206 **Lü JC, Li SX, Ji Q, Wang GF, Zhang JH, Dong ZM. 2006.** New Eusauropod Dinosaur from Yuanmou of Yunnan
1207 Province, China. *Acta Geologica Sinica* **80(1)**:1-10. DOI 10.1111/j.1755-6724.2006.tb00788.x
- 1208 **Lü JC, Li TG, Zhong SM, Ji Q, Li SX. 2008.** A New Mamenchisaurid Dinosaur from the Middle Jurassic of
1209 Yuanmou, Yunnan Province, China. *Acta Geologica Sinica* **82(1)**:17-26. DOI 10.1111/j.1755-
1210 6724.2008.tb00320.x
- 1211 **Madsen JH. 1976a.** *Allosaurus fragilis*: a revised osteology. *Utah Geological and Mineral Survey Bulletin* **109(163)**.
- 1212 **Madsen JH. 1976b.** A second new theropod dinosaur from the Late Jurassic of east central Utah. *Utah Geology*
1213 **3(1)**:51-60.
- 1214 **Madsen JH, Welles SP. 2000.** *Ceratosaurus (Dinosauria, Theropoda) a revised osteology*: Utah Geological Survey,
1215 Miscellaneous Publications 00-2.
- 1216 **Marsh AD, Rowe TB. 2020.** A comprehensive anatomical and phylogenetic evaluation of *Dilophosaurus wetherilli*
1217 (Dinosauria, Theropoda) with descriptions of new specimens from the Kayenta Formation of northern
1218 Arizona. *Journal of Paleontology* **94(S78)**:1-103. DOI 10.1017/jpa.2020.14
- 1219 **Marsh OC. 1881.** Classification of the Dinosauria. *American Journal of Sciences* **23**:81-86.
- 1220 **O'Connor PM. 2007.** The Postcranial Axial Skeleton of *Majungasaurus crenatissimus* (Theropoda: Abelisauridae)
1221 from the Late Cretaceous of Madagascar. *Journal of Vertebrate Paleontology* **27(sup2)**:127-163. DOI

- 1222 10.1671/0272-4634(2007)27[127:Tpasom]2.0.Co;2
- 1223 **Owen R. 1842.** Report on British Fossil Reptiles, Part. II. Report of the eleventh meeting of the British Association
1224 for the advancement of Science, Held at Plymouth in July 1841.
- 1225 **Paul GS. 1988.** Eustreptospondylids and Metriacanthosaurs. In: Cohen IB, Coles R, Dyson F, Feinberg G, Florman
1226 SC, Judson HF, Pagels HR, Pollack RE, Seitz F, Zuckerman H, eds. *Predatory Dinosaurs of the World*. New
1227 York: Simon & Schuster, 286-293.
- 1228 **Pol D, Rauhut OWM. 2012.** A Middle Jurassic abelisaurid from Patagonia and the early diversification of theropod
1229 dinosaurs. *Proc Biol Sci* **279(1741)**:3170-3175. DOI 10.1098/rspb.2012.0660
- 1230 **Rauhut OWM. 2004.** Braincase structure of the Middle Jurassic theropod dinosaur *Piatnitzkysaurus*. *Canadian*
1231 *Journal of Earth Sciences* **41(9)**:1109-1122. DOI 10.1139/e04-053
- 1232 **Rauhut OWM, Bakirov AA, Wings O, Fernandes AE, Hübner TR. 2024.** A new theropod dinosaur from the
1233 Callovian Balabansai Formation of Kyrgyzstan. *Zoological Journal of the Linnean Society* **201(4)**:1-51. DOI
1234 10.1093/zoolinnean/zlae090
- 1235 **Rauhut OWM, Hübner TR, Lanser KP. 2016.** A new megalosaurid theropod dinosaur from the late Middle Jurassic
1236 (Callovian) of north-western Germany: Implications for theropod evolution and faunal turnover in the
1237 Jurassic. *Palaeontologia Electronica* **19.2(26A)**:1-65. DOI 10.26879/654
- 1238 **Rauhut OWM, Pol D. 2019.** Probable basal allosauroid from the early Middle Jurassic Canadian Asfalto Formation
1239 of Argentina highlights phylogenetic uncertainty in tetanuran theropod dinosaurs. *Sci Rep* **9(1)**:18826. DOI
1240 10.1038/s41598-019-53672-7
- 1241 **Sadleir R, Barrett PM, Powell HP. 2008.** *The Anatomy and Systematics of Eustreptospondylus Oxoniensis, A*
1242 *Theropod Dinosaur from the Middle Jurassic of Oxfordshire, England*: Monographs of the
1243 Palaeontographical Society.
- 1244 **Sampson SD, Witmer LM. 2007.** Craniofacial Anatomy of *Majungasaurus crenatissimus* (Theropoda:
1245 Abelisauridae) from the Late Cretaceous of Madagascar. *Journal of Vertebrate Paleontology* **27(sup2)**:32-
1246 104. DOI 10.1671/0272-4634(2007)27[32:CAOMCT]2.0.CO;2
- 1247 **Schade M, Rauhut OWM, Foth C, Moleman O, Evers SW. 2023.** A reappraisal of the cranial and mandibular
1248 osteology of the spinosaurid *Irritator challengeri* (Dinosauria: Theropoda). *Palaeontologia Electronica*
1249 **26(2)**:1-116. DOI 10.26879/1242
- 1250 **Sereno PC, Beck AL, Dutheil DB, Gado B, Larsson HCE, Lyon GH, Marcot JD, Rauhut OWM, Sadleir RW,**
1251 **Sidor CA, Varricchio DD, Wilson GP, Wilson JA. 1998.** A Long-Snouted Predatory Dinosaur from Africa
1252 and the Evolution of Spinosaurids. *Science* **282(5392)**:1298-1302. DOI 10.1126/science.282.5392.1298
- 1253 **Sereno PC, Brusatte SL. 2008.** Basal Abelisaurid and Carcharodontosaurid Theropods from the Lower Cretaceous
1254 Elrhaz Formation of Niger. *Acta Palaeontologica Polonica* **53(1)**:15-46. DOI 10.4202/app.2008.0102
- 1255 **Sereno PC, Dutheil DB, Iarochene M, Larsson HCE, Lyon GH, Magwene PM, Sidor CA, Varricchio DJ, Wilson**
1256 **JA. 1996.** Predatory Dinosaurs from the Sahara and Late Cretaceous Faunal Differentiation. *Science*
1257 **272(5264)**:986-991. DOI 10.1126/science.272.5264.986
- 1258 **Sereno PC, Wilson JA, Larsson HCE, Dutheil DB, Sues HD. 1994.** Early Cretaceous Dinosaurs from the Sahara.
1259 *Science* **266(5183)**:267-271. DOI 10.1126/science.266.5183.267
- 1260 **Smith ND, Makovicky PJ, Hammer WR, Currie PJ. 2007.** Osteology of *Cryolophosaurus ellioti* (Dinosauria:
1261 Theropoda) from the Early Jurassic of Antarctica and implications for early theropod evolution. *Zoological*
1262 *Journal of the Linnean Society* **151(2)**:377-421. DOI 10.1111/j.1096-3642.2007.00325.x

- 1263 **Walker AD. 1964.** Triassic reptiles from the Elgin Area: *Ornithosuchus* and the origin of Carnosaurs. *Philosophical*
1264 *Transactions of the Royal Society of London Series B, Biological Sciences* **248(744)**:53-134.
- 1265 **Wilson JA. 1999.** A nomenclature for vertebral laminae in sauropods and other saurischian dinosaurs. *Journal of*
1266 *Vertebrate Paleontology* **19(4)**:639-653. DOI 10.1080/02724634.1999.10011178
- 1267 **Witmer LM. 1997.** The Evolution of the Antorbital Cavity of Archosaurs: A Study in Soft-Tissue Reconstruction in
1268 the Fossil Record with an Analysis of the Function of Pneumaticity. *Journal of Vertebrate Paleontology*
1269 **17(sup001)**:1-76. DOI 10.1080/02724634.1997.10011027
- 1270 **Wu XC, Currie PJ, Dong ZM, Pan SG, Wang T. 2009.** A new theropod Dinosaur from the middle Jurassic of
1271 Lufeng, Yunnan, China. *Acta Geologica Sinica* **83(1)**:9-24. DOI 10.1111/j.1755-6724.2009.00002.x
- 1272 **Xing LD, Miyashita T, Currie PJ, You HL, Zhang JP, Dong ZM. 2013.** A new basal eusauropod from the Middle
1273 Jurassic of Yunnan, China, and faunal compositions and transitions of Asian sauropodomorph dinosaurs.
1274 *Acta Palaeontologica Polonica* **60(1)**:145-154. DOI 10.4202/app.2012.0151
- 1275 **Xu X, Clark JM, Forster CA, Norell MA, Erickson GM, Eberth DA, Jia CK, Zhao Q. 2006.** A basal
1276 tyrannosauroid dinosaur from the Late Jurassic of China. *Nature* **439(7077)**:715-718. DOI
1277 10.1038/nature04511
- 1278 **You HL, Azuma Y, Wang T, Wang YM, Dong ZM. 2014.** The first well-preserved coelophysoid theropod dinosaur
1279 from Asia. *Zootaxa* **3873(3)**:233-249. 10.11646/zootaxa.3873.3.3
- 1280 **Young CC. 1942.** Fossil vertebrates from Kuangyuan, N. Szechuan (Sichuan), China. *Bulletin of the Geological*
1281 *Society of China* **22(3-4)**:293-309.
- 1282 **Yu YL, Yi HY, Wang SY, Pei R, Zhang C, Xu X. 2023.** A Jurassic Tibetan theropod tooth reveals dental
1283 convergency and its implication for identifying fragmentary fossils. *The Innovation Geoscience* **1(3)**. DOI
1284 10.59717/j.xinn-geo.2023.100040
- 1285 **Zhao XJ, Benson RBJ, Brusatte SL, Currie PJ. 2009.** The postcranial skeleton of *Monolophosaurus jiangi*
1286 (Dinosauria: Theropoda) from the Middle Jurassic of Xinjiang, China, and a review of Middle Jurassic
1287 Chinese theropods. *Geological Magazine* **147(1)**:13-27. DOI 10.1017/s0016756809990240
- 1288 **Zhao XJ, Currie PJ. 1993.** A large crested theropod from the Jurassic of Xinjiang, People's Republic of China.
1289 *Canadian Journal of Earth Sciences* **30(10)**:2027-2036. DOI 10.1139/e93-178

Figure 1

Geographical distribution of metriacanthosaurid theropods in Yunnan, Sichuan, and Chongqing, China.

Each number indicates an individual: 1, *Shidaisaurus jinae*; 2, '*Szechuanosaurus*' *zigongensis*; 3, CNM V214; 4, *Sinraptor hepingensis*; 5 & 6, *Yangchuanosaurus shangyouensis*.

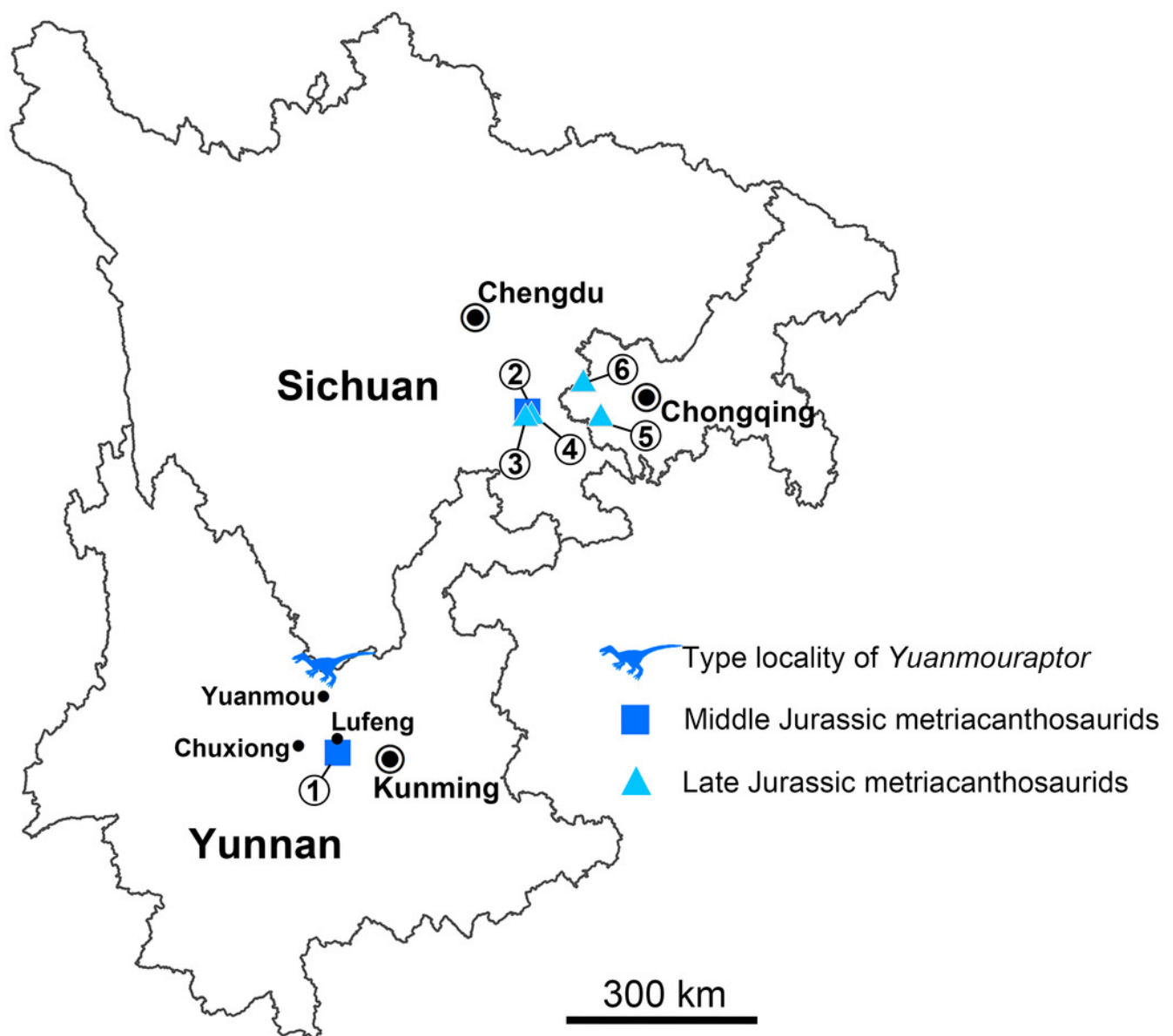


Figure 2

Cranium of *Yuanmouraptor jinshajiangensis* gen. et sp. nov. (LFGT-ZLJ0015).

Cranium in (A) left lateral view with (B) labeled drawing and (C) right lateral view with (D) labeled drawing. Abbreviations: an, angular; ar, articular; bs, basisphenoid; d, dentary; f, frontal, j, jugal; l, lacrimal; lsp; laterosphenoid; m, maxilla; n, nasal; ot, otoccipital; prm, premaxilla; pa, parietal; par, prearticular; pl, palatine; po, postorbital; pop, paroccipital process; pr, prootic; prf, prefrontal; q, quadrate; qj, quadratojugal; sa, surangular; sp, splenial; so, supraoccipital; sq, squamosal. Striated area indicates damage and grey area indicates matrix. Scale bar represents 100 mm. Photos by Xiao-Chun Wu.

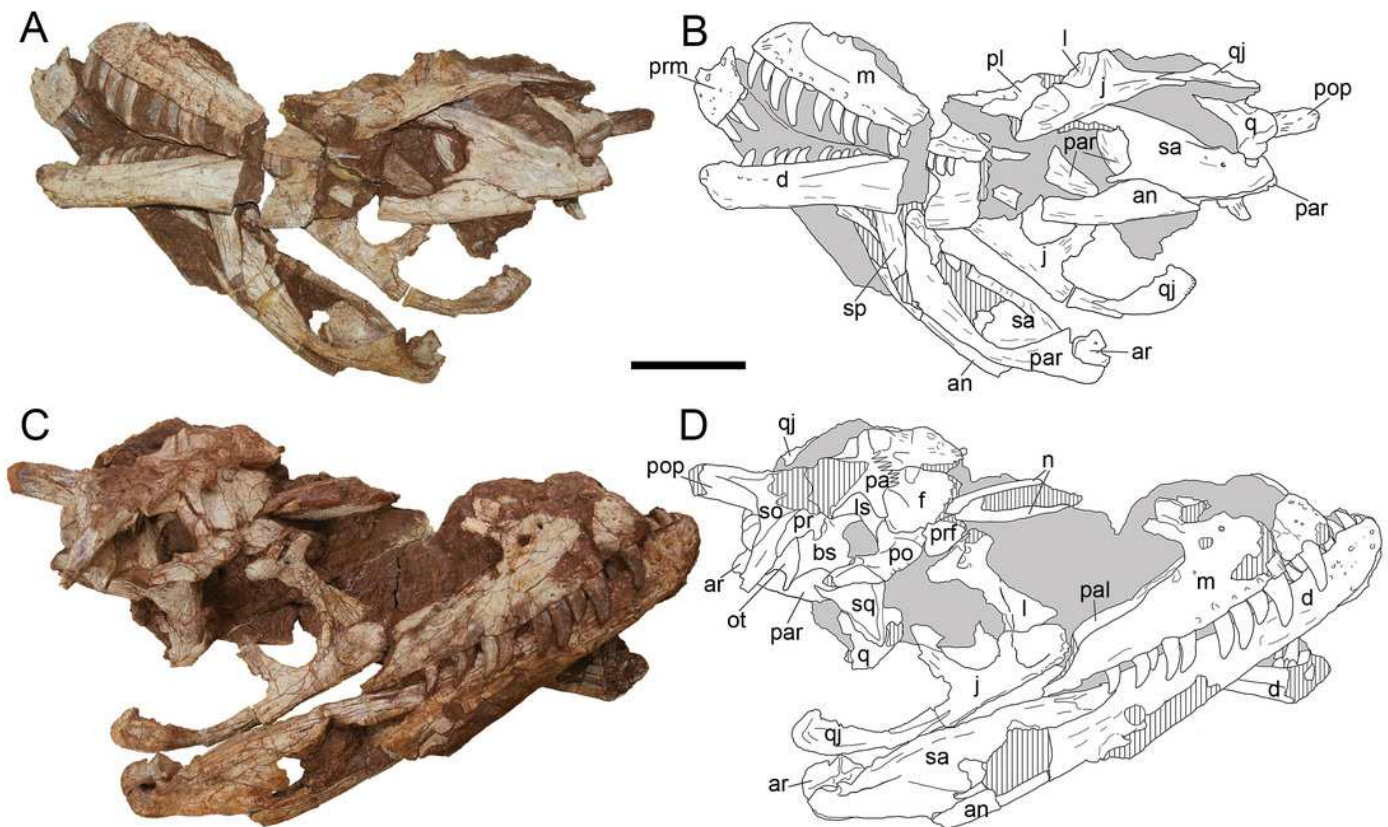


Figure 3

Reconstruction of the cranium of *Yuanmouraptor jinshajiangensis* gen. et sp. nov. (LFGT-ZLJ0015).

Abbreviations: an, angular; bs, basisphenoid; d, dentary; emf, external mandibular fenestra; j, jugal; l, lacrimal; m, maxilla; ot, otoccipital; prm, premaxilla; par, prearticular; pl, palatine; po, postorbital; pop, paroccipital process; pr, prootic; prf, prefrontal; q, quadrate; qj, quadratojugal; sa, surangular; sq, squamosal. Shaded area indicates the missing part, and dashed line marks the margin of breakage of bone. Scale bar represents 100 mm.

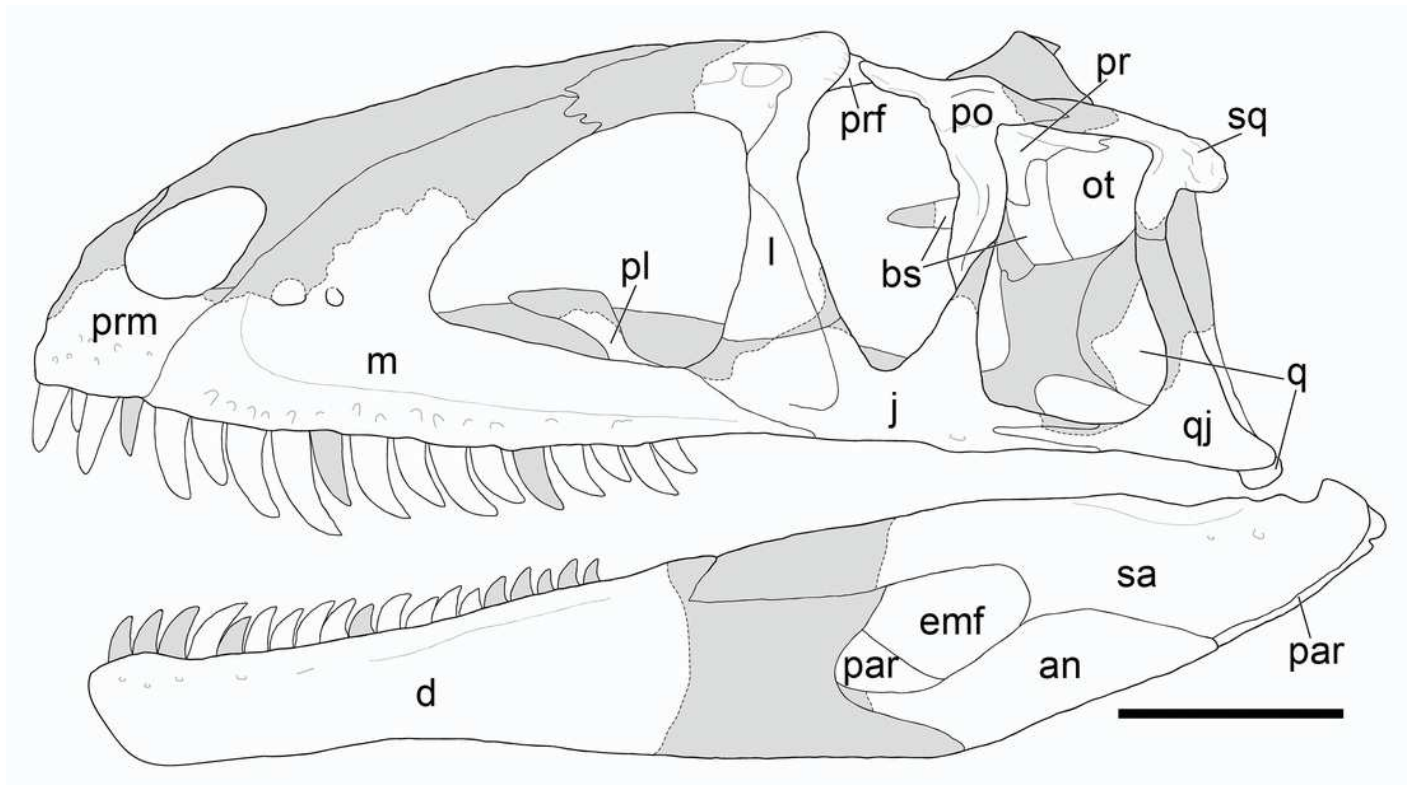


Figure 4

Premaxilla and maxilla of *Yuanmouraptor jinshajiangensis* gen. et sp. nov. (LFGT-ZLJ0015).

Left premaxilla in (A) lateral view with (B) labeled drawing. (C) Serration on the premaxillary teeth, with mesial carina pointed by white arrows. (D) Serration on the mesial and distal carina of the maxillary teeth. Left maxilla in (E) lateral view with (F) labeled drawing. Right maxilla in (G) lateral view with (H) labeled drawing. Abbreviations: aof, antorbital fossa; aofe, antorbital fenestra; asr, remnant ascending ramus of maxilla; en, external naris; mc, maxillary contact; mf, maxillary fenestra; m1-14, maxillary teeth 1-14; nf, narial fossa; np, nasal process; pmf, promaxillary fenestra; prc, premaxillary contact. p1-3, premaxillary teeth 1-3; sn, subnarial process. Striated area indicates damage. Scale bars for A-B present 50 mm, for C-D, 5 mm, and for E-H, 100 mm. Photos by Xiao-Chun Wu and Yi Zou.

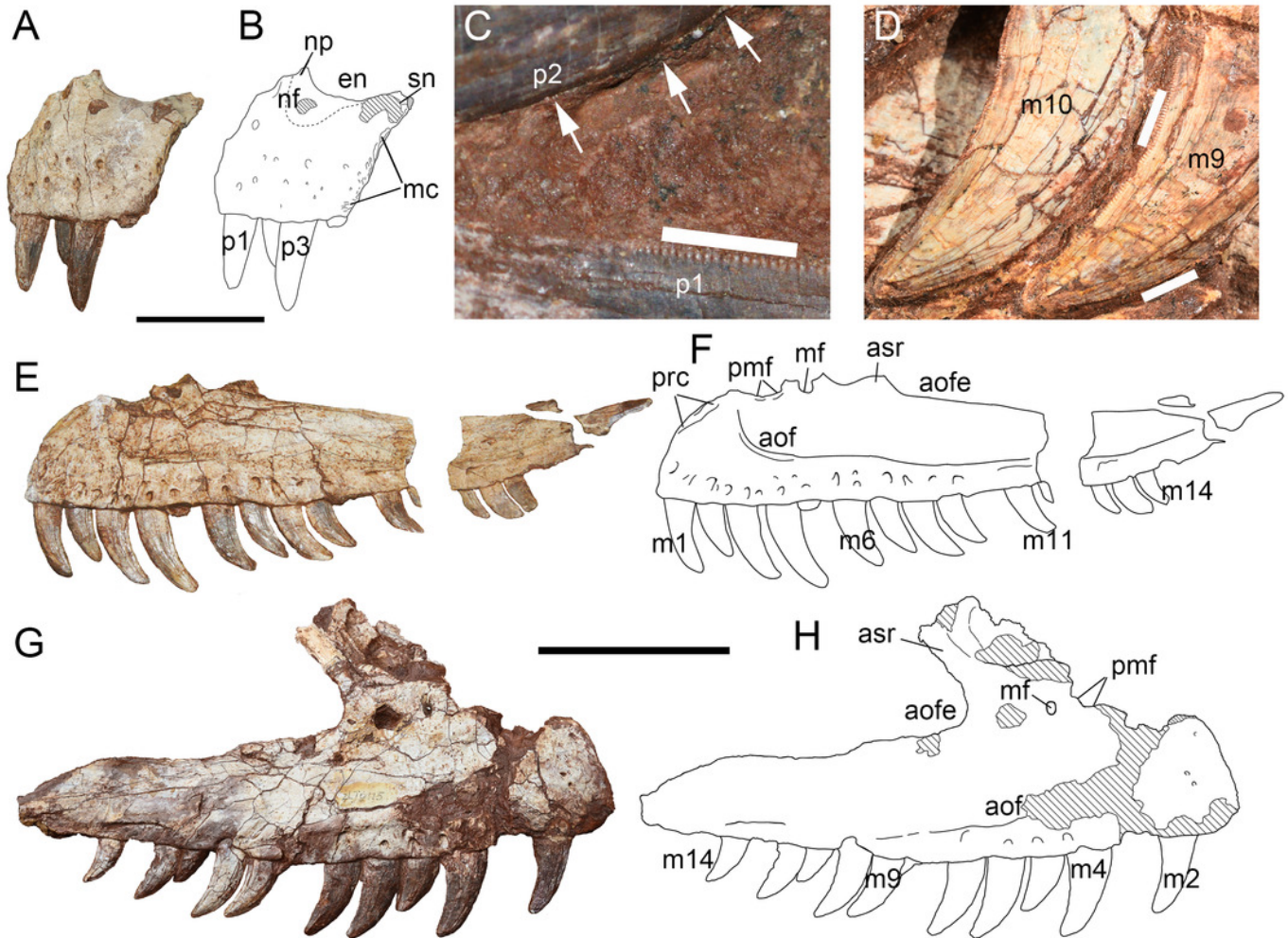


Figure 5

Skull elements of *Yuanmouraptor jinshajiangensis* gen. et sp. nov. (LFGT-ZLJ0015).

Right lacrimal in (A) lateral view with (B) labeled drawing. Articulated right jugal and quadratojugal in (C) lateral view with (D) labeled drawing. Articulated right jugal and quadratojugal in (E) medial view with (F) labeled drawing. Left jugal in (G) lateral view with (H) labeled drawing. (I) Left quadratojugal and partial quadratojugal ramus of left jugal. Abbreviations: aof, antorbital fossa; de, depression; f, flange; fo, fossa; j, jugal; lc, lacrimal contact; lla, lateral lamina; ltf, lateral temporal fenestra; mla, medial lamina; o, orbit; pn, pneumatic foramen; por, postorbital ramus of jugal; qj, quadratojugal; qjr, quadratojugal ramus of jugal. Striated areas indicate damage. Scale bars present 50 mm. Photos by Xiao-Chun Wu and Yi Zou.

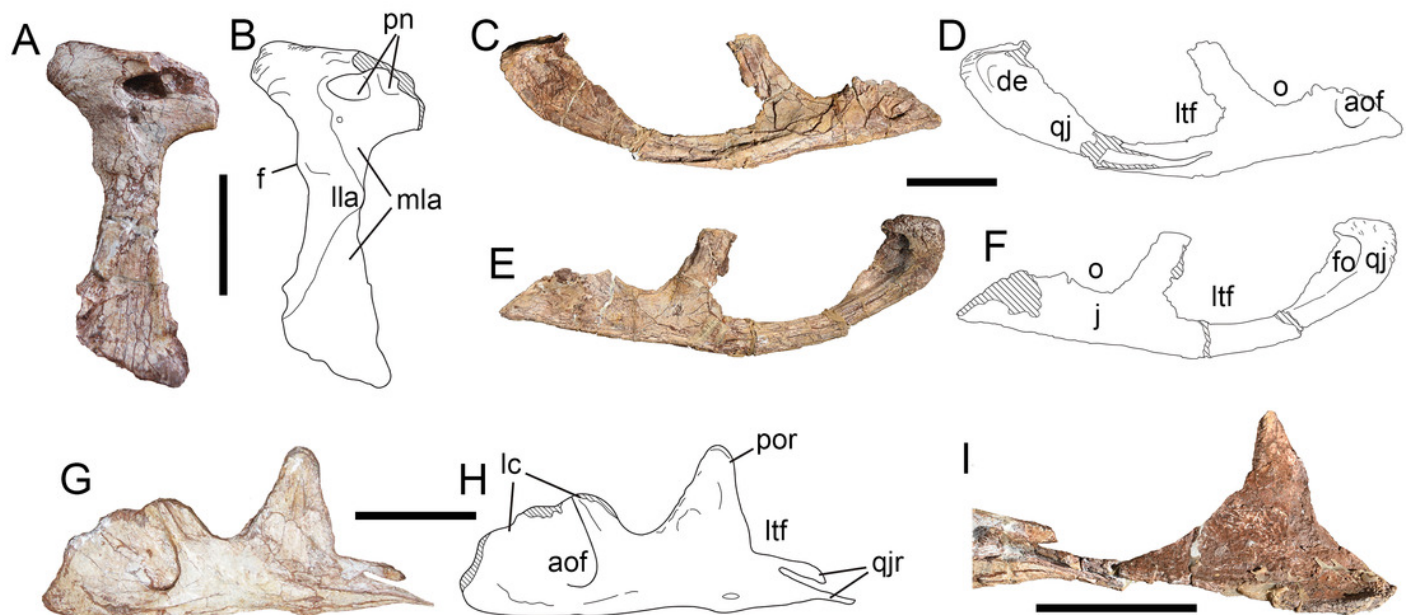


Figure 6

Postorbital and skull roof of *Yuanmouraptor jinshajiangensis* gen. et sp. nov. (LFGT-ZLJ0015)

Right postorbital in (A) lateral view with (B) labeled drawing, and in (C) posterior view with (D) labeled drawing. Skull roof in (E) dorsal view with (F) labeled drawing. Abbreviations: de, depression; f, frontal; l, lacrimal; la, lamina; lsp, laterosphenoid; n, nasal; or, orbital ramus; ot, otoccipital; pa, parietal; po, postorbital; pop, paroccipital process; por, posterior ramus; pr, prootic; prf, prefrontal; r, ridge; so, supraoccipital; stf, supratemporal fenestra; stfo, supratemporal fossa; t, trough; vr, ventral ramus of postorbital. Striated area indicates damage and grey area indicates matrix. Scale bars present 50 mm. Photos by Xiao-Chun Wu.

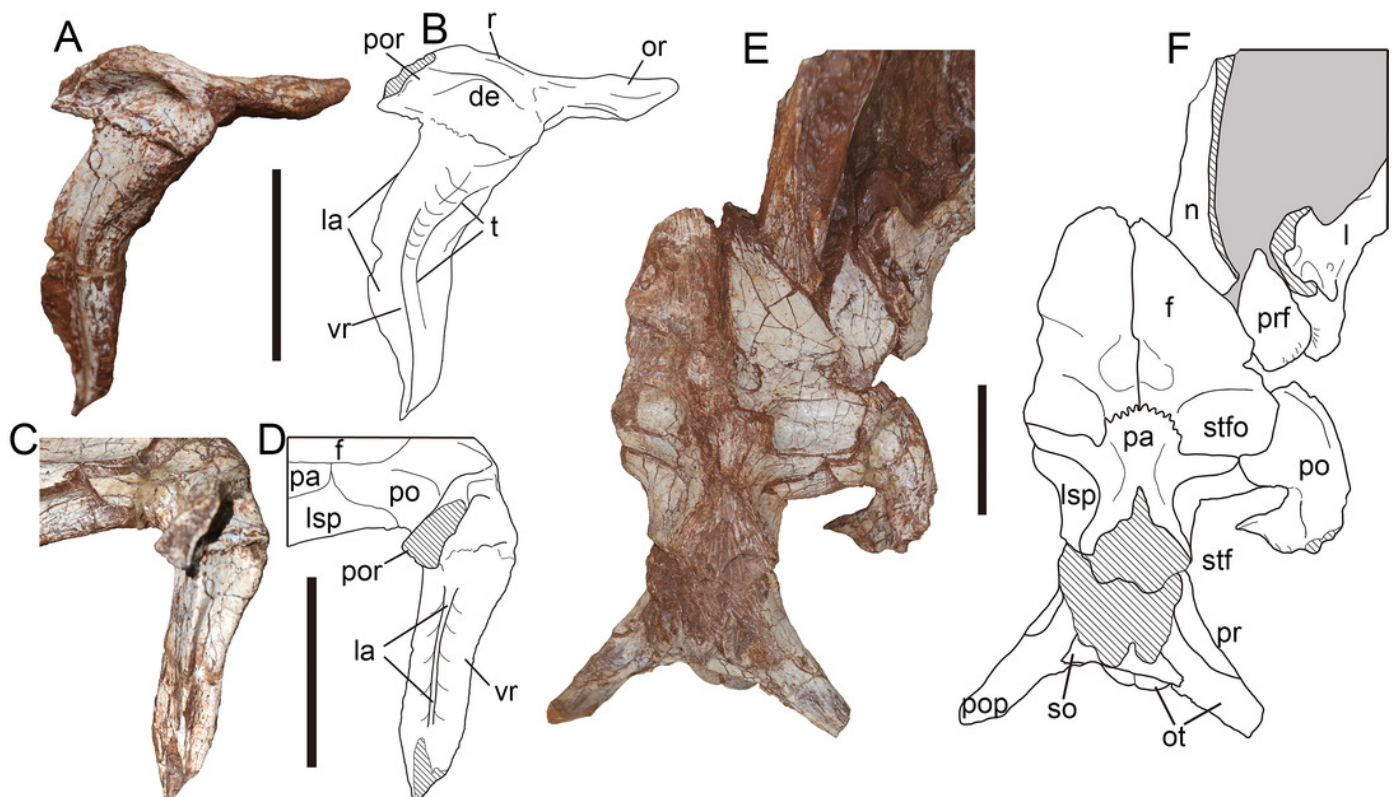


Figure 7

Skull elements of *Yuanmouraptor jinshajiangensis* gen. et sp. nov. (LFGT-ZLJ0015).

Right squamosal in (A) dorsal view with (B) labeled drawing, in (C) posterodorsal view with (D) labeled drawing, and in (E) lateral view. Left quadrate in (F) anterolateral, (G) posterolateral, and (H) ventral views. Left palatine in (I) lateral view with (J) labeled drawing. Abbreviations: ap, anterior process; ecc, ectocondyle; enc, entocondyle; ics, intercondylar sulcus; in, internal naris; ltf, lateral temporal fenestra; mp, medial process; map, maxillary process; pac, parietal contact; po, postorbital; popc, paroccipital process contact; pn, pneumatic foramen; pp, posterior process; qc, contact for quadrate; qs, quadrate shaft; r, ridge; vp, ventral process; vptp, vomeropterygoid process. Striated area indicates damage and grey area indicates matrix. Scale bar presents 50 mm. Photos by Xiao-Chun Wu and Yi Zou.

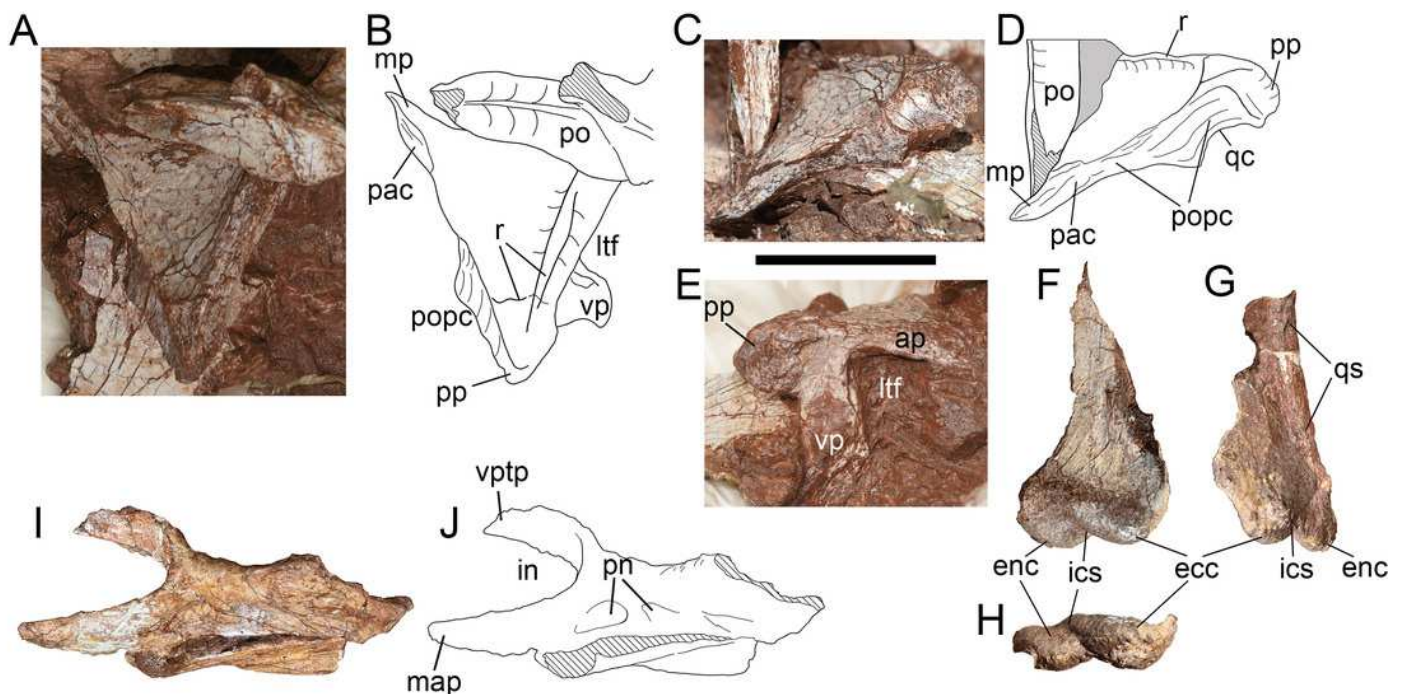


Figure 8

Occiput of *Yuanmouraptor jinshajiangensis* gen. et sp. nov. (LFGT-ZLJ0015).

Supraoccipital and adjacent bones in (A) posterodorsal view with (B) labeled drawing. (C) Depression housing cranial nerves. Braincase in (D) posterior view with (D) labeled drawing. Abbreviations: bo, basioccipital; bs, basisphenoid; eo, exoccipital; fm, foramen magnum; oc, occipital condyle; op, opisthotic; pop; paroccipital process; r, ridge; so, supraoccipital; vcd, foramen vena capitis dorsalis; X, X(I) XI(I) foramina for cranial nerves; ?, unknown bone. Striated area indicates damage. Scale bar presents 50 mm. Photos by Xiao-Chun Wu.

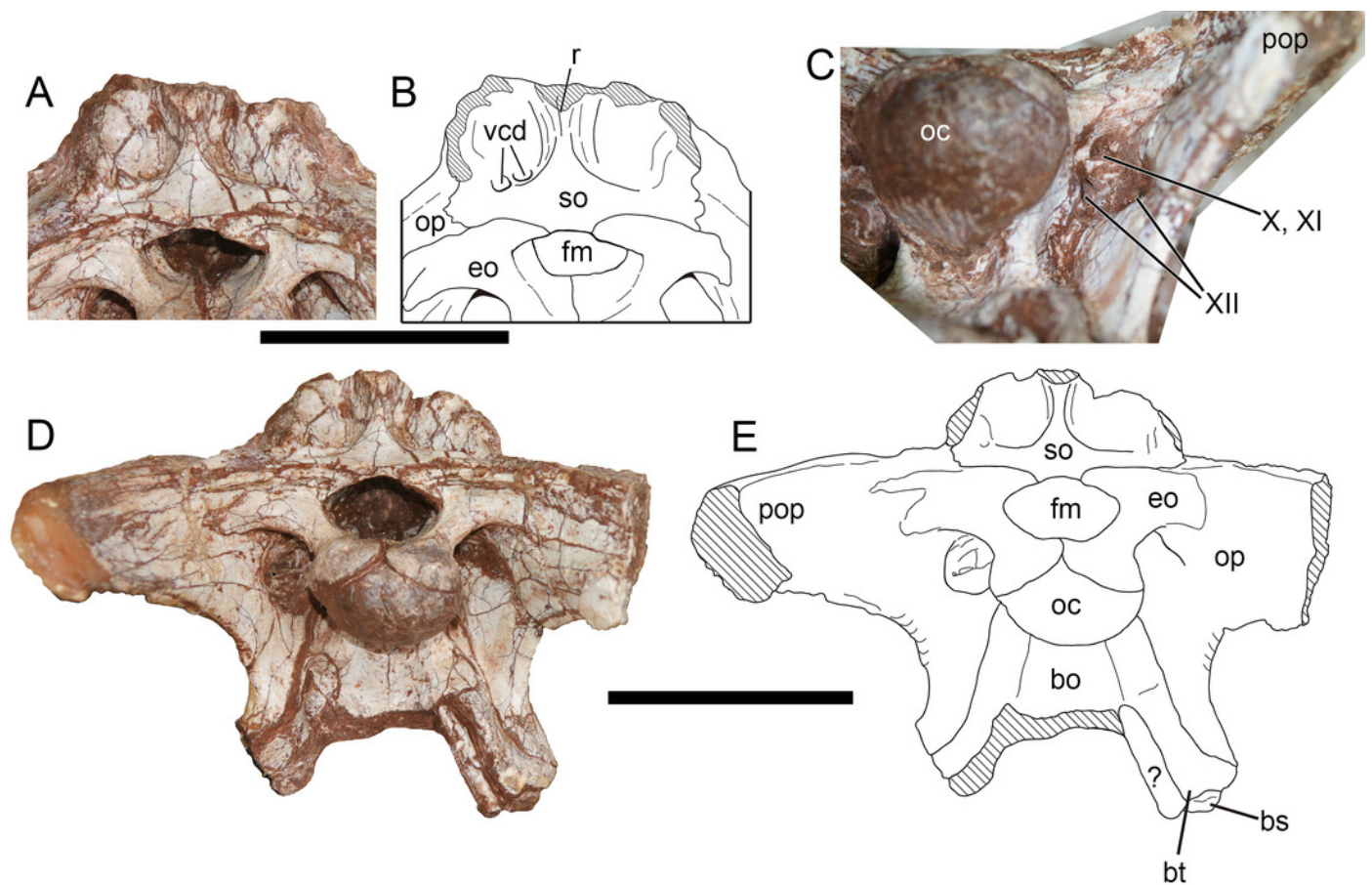


Figure 9

Braincase of *Yuanmouraptor jinshajiangensis* gen. et sp. nov. (LFGT-ZLJ0015).

Braincase in (A) lateroposterior view with (B) labeled drawing and in (C) laterodorsal view with (D) labeled drawing. Abbreviations: bo, basioccipital; bs, basisphenoid; bt, basal tuber; cfp, cultriform process; cp, crista prootica; fo, fenestra ovalis; lsp, laterosphenoid; oc, occipital condyle; op, opisthotic; pa, parietal; po, postorbital; pop, paroccipital process; pp, prootic pendant; pr, prootic; vcd, foramen vena capitis dorsalis; VI(I) cranial nerve VII (facial nerve); so, supraoccipital. Straited area inidcates damage and grey area indicates matrix. Scale bar presents 50 mm. Photos by Xiao-Chun Wu.

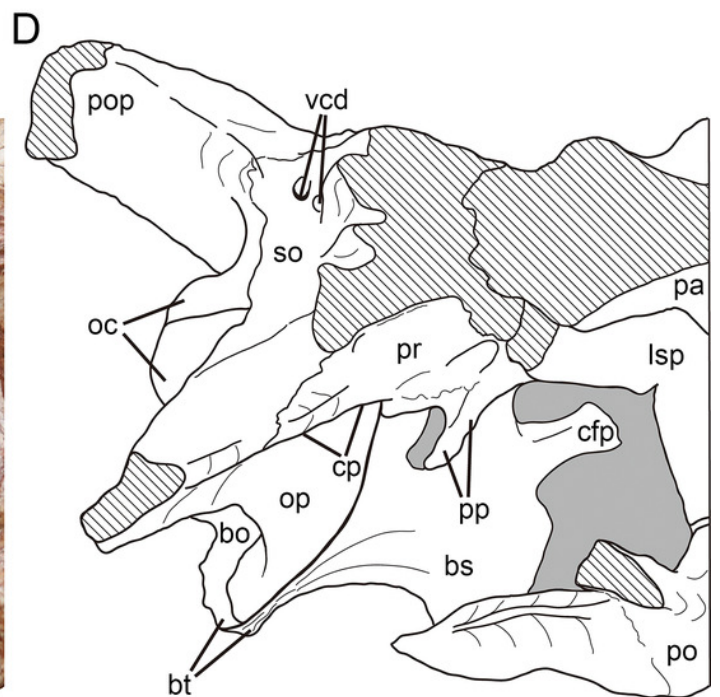
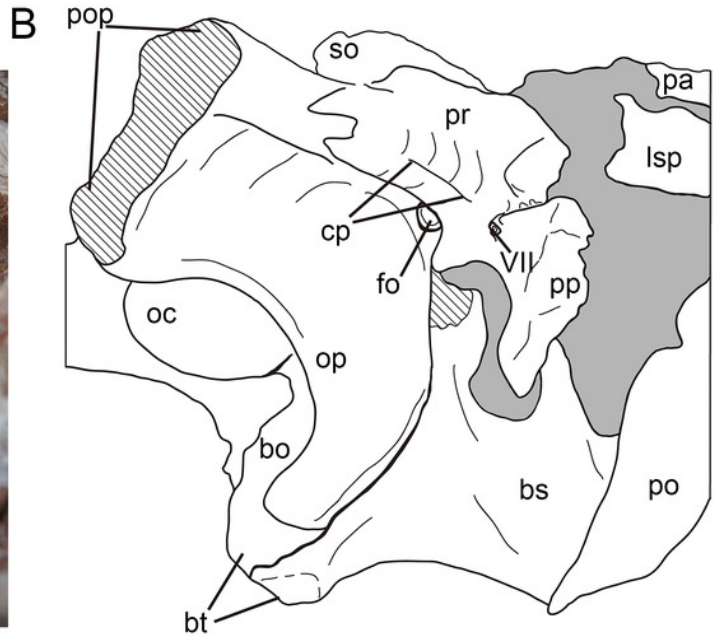
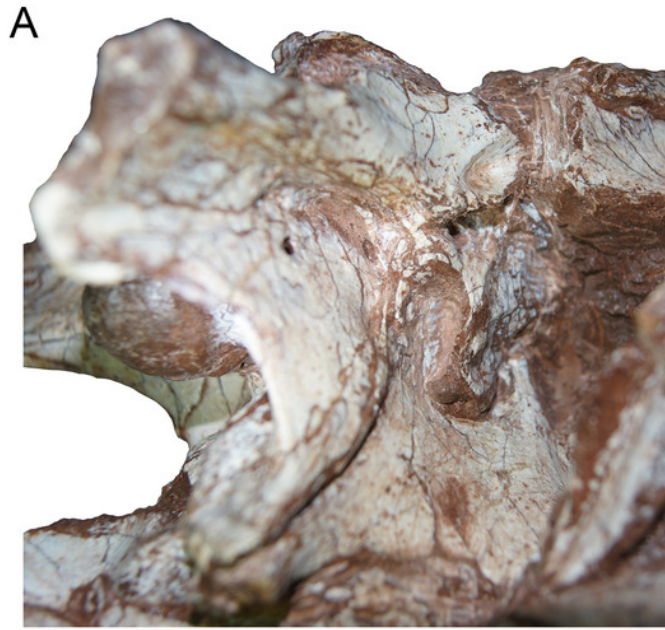


Figure 10

Mandibular elements of *Yuanmouraptor jinshajiangensis* gen. et sp. nov. (LFGT-ZLJ0015).

Left dentary in (A) lateral view with (B) labeled drawing. Left posterior part of mandible in (C) lateral view with (D) labeled drawing. Right posterior part of mandible in (E) medial view with (F) labeled drawing. Abbreviations: af, adductor fossa; an, angular; ar, articular; ct, foramen of condra typamni; d4-14, dentary teeth 4-14; emf, external mandibular fenestra; g, groove; hp, hook like process of surangular; imf, internal mandibular fenestra; lg, lateral glenoid; mame, attachment of M. adductor mandibulae externus; nf, neurovascular foramina. par, prearticular; psf, posterior surangular foramen; retp, retroarticular process; sa, surangular; sp, splenial; sr, surangular ridge. Striated area indicates damage. Scale bar presents 50 mm. Photos by Xiao-Chun Wu and Yi Zou.

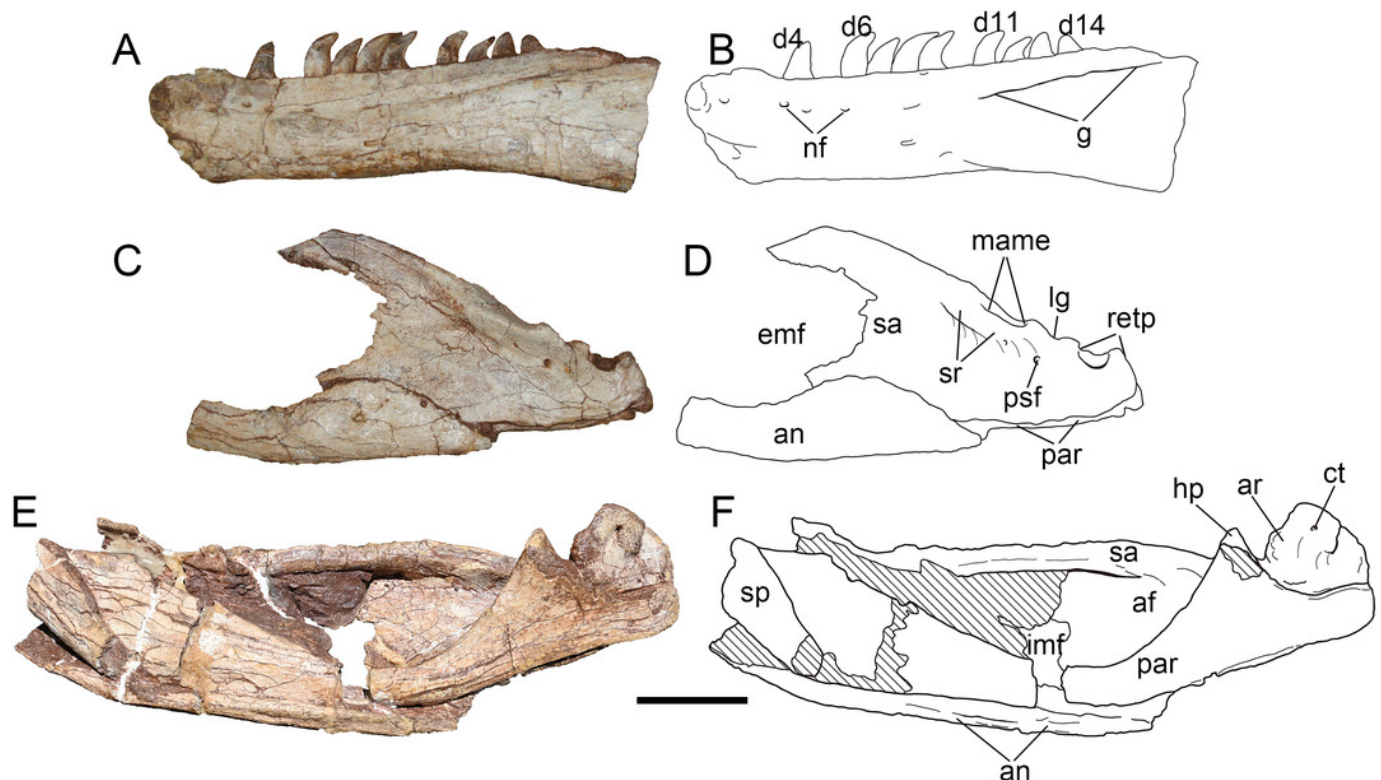


Figure 11

Mandibular joint of *Yuanmouraptor jinshajiangensis* gen. et sp. nov. (LFGT-ZLJ0015).

Right mandibular joint in (A) lateral view with (B) labeled drawing and in (C) dorsal view with (D) labeled drawing. Abbreviations: ar, articular; ct, foramen of condra typani; hp, hook like process of surangular; lg, lateral glenoid; mame, attachment of M. adductor mandibulae externus; mg, medial glenoid; par, prearticular; psf, posterior surangular foramen; r, ridge; retp, retroarticular process; sa, surangular; sr, surangular ridge. Scale bar presents 50 mm. Photos by Xiao-Chun Wu and Yi Zou.

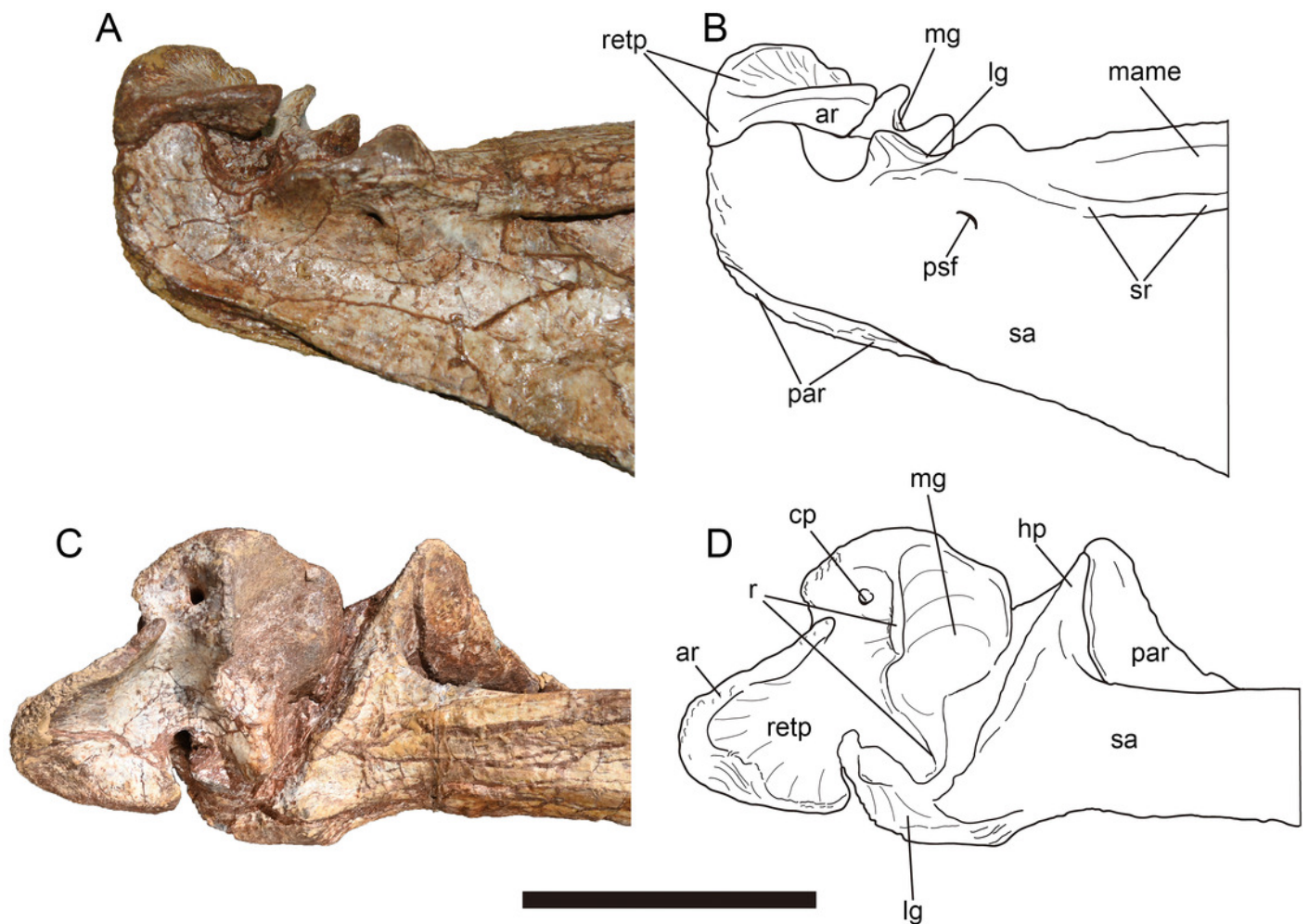


Figure 12

Atlas-axis complex of *Yuanmouraptor jinshajiangensis* gen. et sp. nov. (LFGT-ZLJ0115).

Atlas-axis complex in ((A)), dorsal, (B) ventral, (C) anterior, (D) posterior, (E) right lateral and (F) left lateral views. Abbreviations: ati, atlantal intercentrum; axi, axial intercentrum; dp, diapophysis; ep, epipophysis; na, neurapophysis; nc, neural canal; od, odontoid; poz, postzygopophysis; pp, parapophysis; re, rounded eminence; spol, spinopostzygipophyseal lamina; tpol, intrapostzygopophyseal lamina. All names of the bony laminae follow terminologies in *Wilson (1999)*. Scale bar presents 50 mm. Photos by Xiao-Chun Wu.

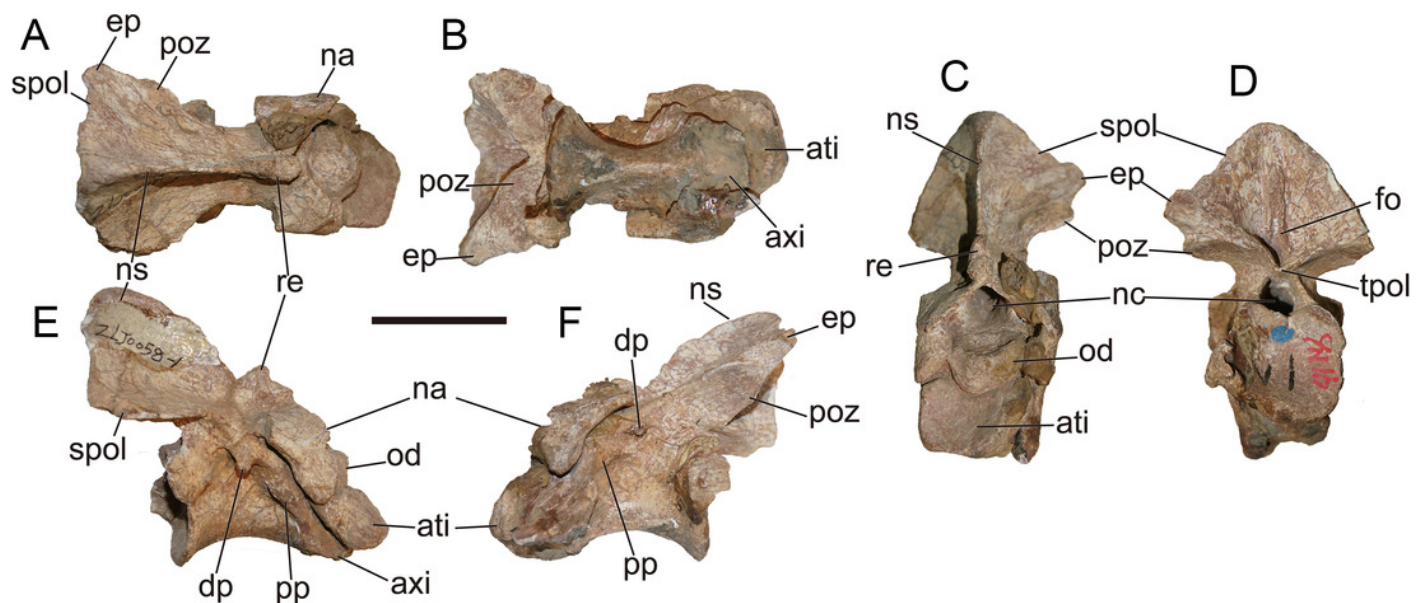


Figure 13

Postaxial vertebrae of *Yuanmouraptor jinshajiangensis* gen. et sp. nov. (LFGT-ZLJ0115).

Postaxial vertebrae in lateral view. (A) Cervical 3; (B) Cervical 4; (C) Cervical 5; (D) Cervical 6; (E) Cervical 7; (F) Cervical; (G) Cervical 9; (H) Cervical 10; (I) Dorsal 1. Abbreviations: acdl, anterior centrodiapophyseal lamina; cpol, centropostzygopophyseal lamina; cpri, centroprezygopophyseal lamina; dp, diapophysis; ep, epiphysis; ns, neural spine; pcld, posterior centrodiapophyseal lamina; pl, pleurocoel; podl, postzygodiapophyseal lamina; poz, postzygopophysis; pp, parapophysis; prdl, prezygodiapophyseal lamina; prz, prezygopophysis; spol, spinopostzygopophyseal lamina; ri, distinct rim on the anterior articular surface; sprl, spinoprezygodiapophyseal lamina; vk, ventral keel. All names of the bony laminae follow terminologies in *Wilson (1999)*. Scale bar presents 50 mm. Photos by Xiao-Chun Wu.

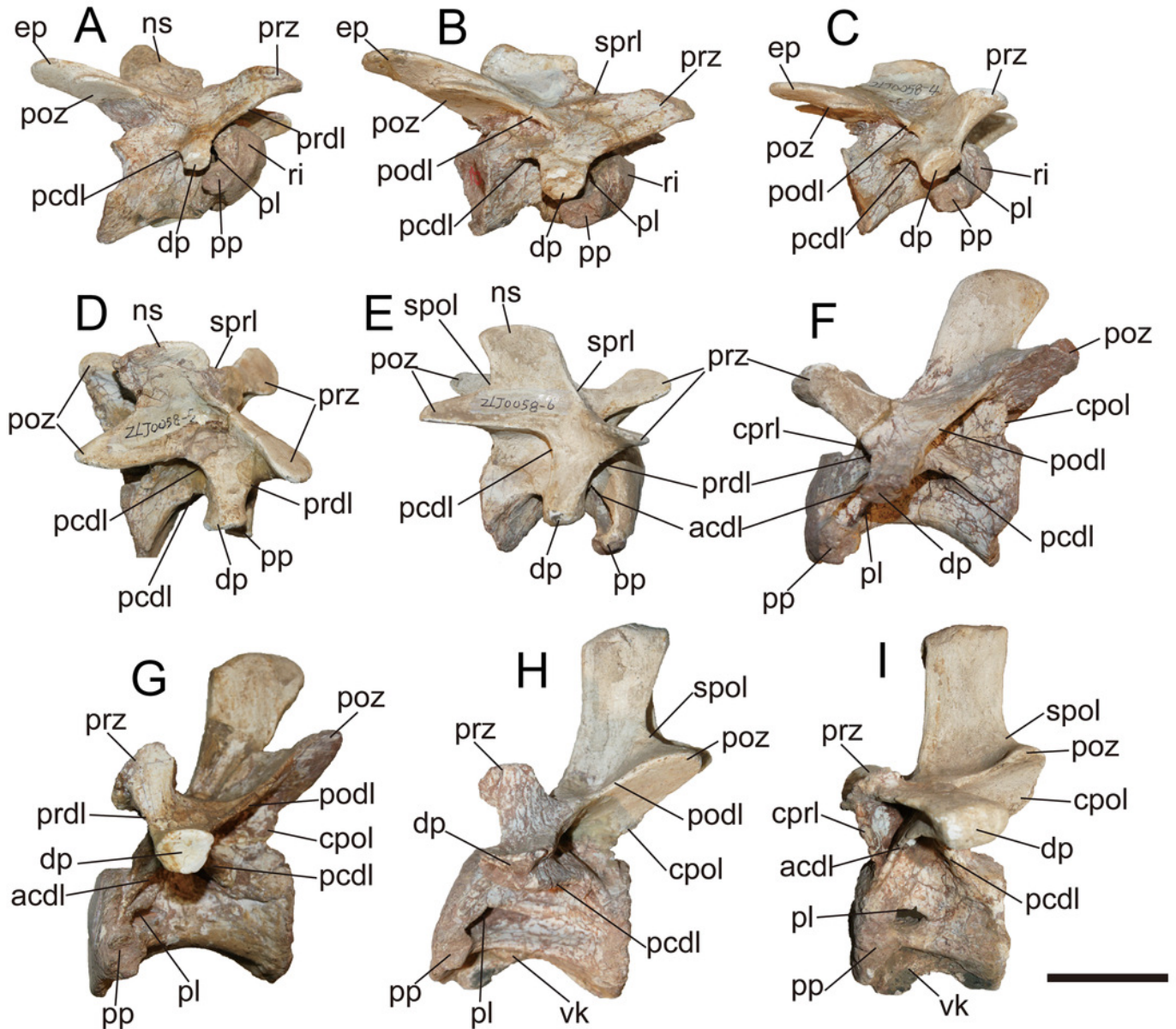


Figure 14

Postaxial vertebrae of *Yuanmouraptor jinshajiangensis* gen. et sp. nov. (LFGT-ZLJ0115).

Cervical 3 in (A) anterior, (B) posterior, (C) ventral, (D) dorsal views. Cervical 5 in (E) ventral, (F) posterior views. Cervical 9 in (G) anterior, (H) posterior, (I) dorsal views. Abbreviations: cpol, centropostzygopophyseal lamina; cpri, centroprezygopophyseal lamina; ep, epiphysis; nc, neural canal; ns, neural spine; pl, pleurocoel; podl, postzygodiapophyseal lamina; poz, postzygopophysis; prz, prezygodiapophyseal lamina; ri, distinct rim on the anterior articular surface; tpol, intrapostzygopophyseal lamina; tpri, intraprezygopophyseal lamina; spol, spinopostzygopophyseal lamina. All names of the bony laminae follow terminologies in *Wilson (1999)*. Scale bar presents 50 mm. Photos by Xiao-Chun Wu.

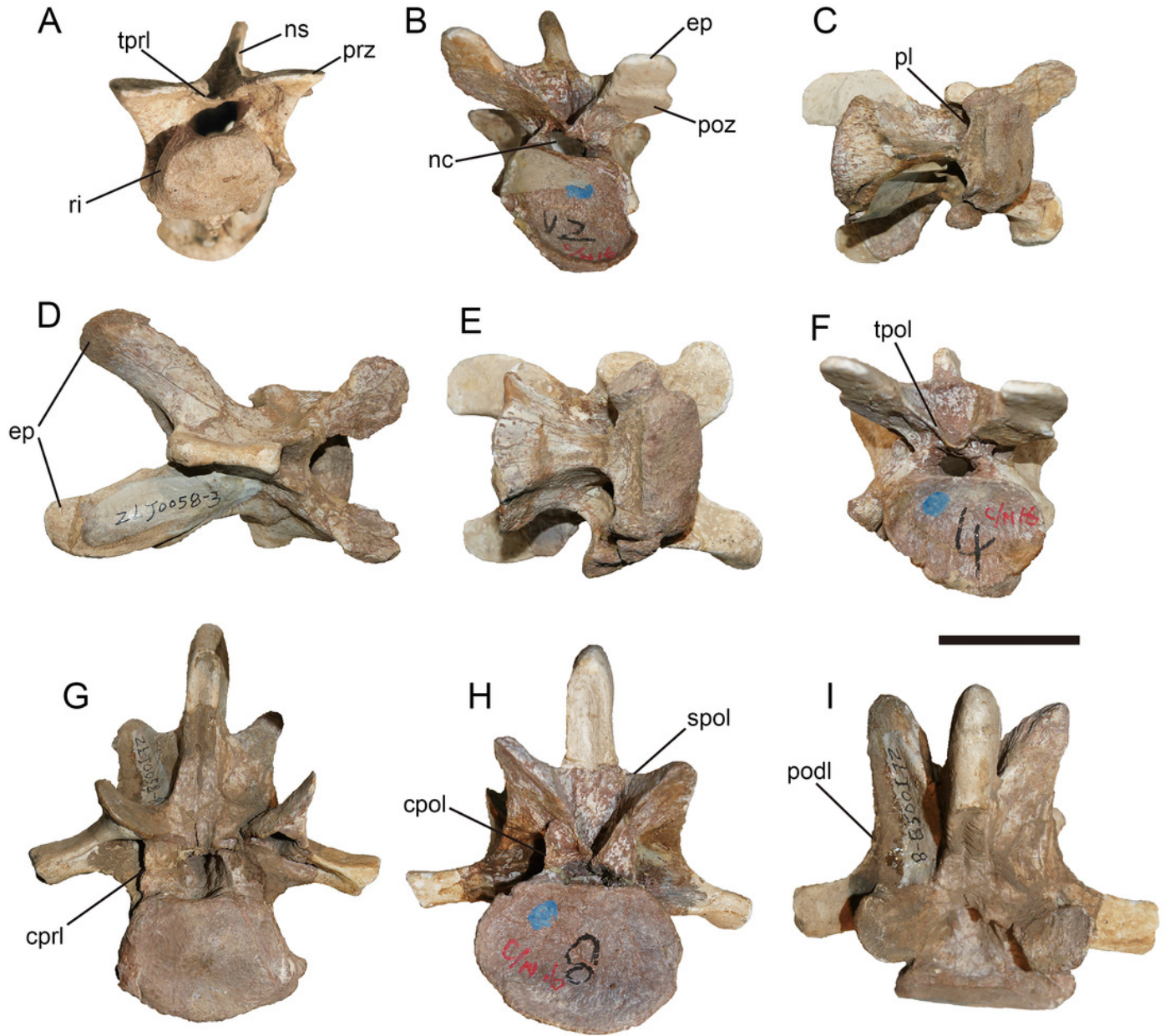


Figure 15

Result of phylogenetic analysis

Time-Calibrated strict consensus tree showing the phylogenetic position of *Yuanmouraptor* with the latest geological time scale.

